SEARCH-BASED VS. TASK-BASED SPACE SURVEILLANCE FOR GROUND-BASED TELESCOPES

THESIS

Fred D. Hertwig, MS, Captain, USAF

AFIT-ENV-MS-19-M-178

DEPARTMENT OF THE AIR FORCE
AIR UNIVERSITY

AIR FORCE INSTITUTE OF TECHNOLOGY

Wright-Patterson Air Force Base, Ohio

AFIT-ENV-MS-19-M-178

SEARCH-BASED VS. TASK-BASED SPACE SURVEILLANCE FOR GROUND-BASED TELESCOPES

THESIS

Presented to the Faculty

Department of Systems Engineering & Management

Graduate School of Engineering and Management

Air Force Institute of Technology

Air University

Air Education and Training Command

In Partial Fulfillment of the Requirements for the

Degree of Master of Science in Systems Engineering

Fred D. Hertwig, MS

Captain, USAF

March 2019

AFIT-ENV-MS-19-M-178

SEARCH-BASED VS. TASK-BASED SPACE SURVEILLANCE FOR GROUND-BASED TELESCOPES

Fred D. Hertwig, MS

Captain, USAF

Committee Membership:

Dr. John M. Colombi
Chair

Dr. Richard G. Cobb
Member

Mr. David W. Meyer
Member

Abstract

Persistent Space Situational Awareness (SSA) is one of the top priorities of the DoD. Currently the Space Surveillance Network (SSN) operates using only a task-based method. The goal of this thesis was to compare the current task-based space surveillance performance to a search-based method of space surveillance in the GEO belt region. The performance of a ground telescope network, similar to the Ground-Based Electro-Optical Deep Space Surveillance (GEODSS) network, was modeled and simulated using AGI's Systems Tool Kit (STK) and Python. The model compared search-based and task-based space surveillance methods by simulating 813 Resident Space Objects (RSOs) on the summer solstice, fall equinox and winter solstice. Four performance metrics for comparing the search-based and task-based methods were minimum detectable size, detection rate, coverage area, and latency. The search-based method modeled six different search patterns at varying starting positions. Results show that the minimum detectable size average for task-based was 47.6 cm in diameter while search-based methods ranged from 38.3 cm - 45.4 cm in diameter. Detection rate for task-based was 100% while the search-based ranged from 91.7% - 96.8%. Coverage area for task-based was 46% of the GEO belt and the search-based method ranged from 3.5% - 84.4%. Average latency (revisit time) for task-based was 78 minutes and search-based methods ranged from 62 - 469 minutes. It was found that task-based surveillance was the better method for current operational conditions by using a weighted decision criteria. However, as the number of RSOs increase there is a point at which the search method has better performance.

Acknowledgments

I would like to express my sincere appreciation to my faculty advisor, Dr. John M. Colombi and my committee, for their guidance and support throughout the course of this thesis effort. The encouragement and insight they provided was instrumental through the past year. I would also like to thank Maj Grant Thomas for providing LEEDR transmission curves, Bob Bruck at GEODSS Det 3 for his technical guidance, the GEODSS program office for helping scope the thesis and the 18th SPCS for providing data and answering questions. I would like to thank Analytical Graphics Incorporated for the educational use of their STK Engine. Most importantly, I would like to thank my wife for the love and support during this endeavor and providing professional Microsoft Word editing skills.

Fred D. Hertwig

Table of Contents

Page

List of Figures

Page

List of Tables

Page

List of Acronyms

AFSPC	Air Force Space Command
AFRL	Air Force Research Laboratory
AGI	Analytical Graphics Inc.
BDD	Block Definition Diagram
CT	Correlated Tracks
DoD	Department of Defense
DOTS	Dynamic Optical Telescope System
ESA	European Space Agency
FOV	Field-Of-View
GEO	Geosynchronous Orbit
GEODSS	Ground-Based Electro-Optical Deep Space Surveillance
GPO	Geosynchronous Polar Orbit
GSSAP	Geosynchronous Space Situational Awareness Program
HEO	Highly Elliptical Orbit
INCOSE	International Council on Systems Engineering
ISON	International Scientific Optical Network
JP	Joint Publication
JSpOC	Joint Space Operations Center
LEEDR	Laser Environmental Effects Definition Reference
LEO	Low Earth Orbit
MBSE	Model Based Systems Engineering

MEO	Medium Earth Orbit
MODEST	Michigan Orbital Debris Survey Telescope
M&S	Modelling and Simulation
NASA	National Air and Space Agency
PAN-STARRS	Panoramic Survey Telescope and Rapid Response System
RA	Right Ascension
RPO	Rendezvous and Proximity Operations
SBSS	Space Based Space Surveillance
SE	Systems Engineering
SNR	Signal to Noise Ratio
SSA	Space Situational Awareness
SSN	Space Surveillance Network
SST	Space Surveillance Telescope
STK	Systems Tool Kit
SysML	Systems Modeling Language
TASMAN	Tasking of Autonomous Sensors in a Multiple Application Network
TLES	Two Line Element Sets
UCT	Uncorrelated Track
US	United States
WENESSA	Wide Eye-Narrow Eye Space Simulation for Situational Awareness
WSF	Defense Weather System Follow-on

I. Introduction

General Issue

Operations in space are congested, contested and competitive (JP 3-14, 2018). In the past few decades, even countries with minimal technology advancement have been able to gain access to space. Civilian entities have also been able to increase their presence in the space domain adding to the congested, contested and competitive environment (Coats, 2018). The United States (US) no longer has the luxury of operating in space without hindrance. Threats to US space operations can be put into two categories; natural hazards and man-made threats. Natural hazards include solar activity, radiation, and orbital debris that can degrade or destroy a satellite. Man-made threats include jamming from the ground or another satellite, cyber-attacks, anti-satellite weapons, and disruptive/destructive enemy space vehicles (JP 3-14, 2018). Both natural and man-made threats can render a satellite useless adding to the population of space debris, exacerbating the problem. The US must have persistent Space Situational Awareness (SSA) to be able to detect and track threats to their operations; "Situational awareness is fundamental to conducting space operations. SSA is the requisite foundational, current, and predictive knowledge and characterization of space objects" (JP 3-14, 2018).

Problem Statement

The current US Space Surveillance Network (SSN) needs to be able to better detect maneuvering enemy satellites and proximity operations in the Geosynchronous Orbit (GEO) belt at all times. GEO is defined as an orbit at an altitude of about 35,780

km and the same 24-hour period as the Earth's rotation. The orbit region allows for a constant line of sight and coverage of roughly one-third of the earth with a single satellite which is key for worldwide communication, surveillance, tracking large weather patterns and missile warning (JP 3-14, 2018). The SSN also must be able to detect space debris that could potentially cause a collision and damage or destroy operational satellites.

In task-based surveillance, a list of unique taskings are sent to each surveillance site from the Combined Space Operations Center (CSpOC)[1]. The site then performs those taskings by taking images or observations of individual objects in space. The observations are then returned to the JSpOC. Images are only taken from the task list received by the site. This leaves windows of opportunity for enemy satellites to maneuver without detection or allows an accidental collision with space debris without warning. The current tasked-based process of tracking satellites leaves portions of the GEO belt un-viewed either for long periods of time or never viewed at all. Small area searches do occur when the expected object is not in the first field-of-view (FOV).[2] However, only a few observations are taken around where the object is expected to be in its orbit. No full sky searches are currently being conducted. Nightly surveying or searching of the GEO belt could increase the probability of detection of enemy movements and orbiting space debris. In search-based space surveillance, the site would image the entire viewable sky each night and not be limited to the predetermined tasks sent by the JSpOC.

[1] The JSpOC transitioned to the CSpOC in July 2018
[2] FOV is the area of the sky that the telescope can observe with one exposure.

Research Purpose/Questions

The purpose of this research is to investigate how switching to a 100% search-based space surveillance approach would affect space surveillance performance when compared with the current task-based approach. Adding new surveillance assets like ground telescopes and observation satellites would certainly increase performance of the SSN, but may not be cost effective. Possible low-cost benefits could be found by simply changing the way GEO observations are accomplished. Answering these specific research questions could provide a possible solution.

1. How does switching from tasked-based to search-based space surveillance affect GEO SSA performance for a simulated ground-based telescope network?
2. How do different search patterns and constraints affect performance?

The JSpOC measures ground telescope system performance by the rate of successfully acquired tasked tracks and has in the past used tasking response time. However to compare task-based and search-based methods additional metrics will be used. For this thesis, latency will act as a surrogate for response time and detection rate will be a surrogate for the rate of successfully acquired tasked tracks. In addition, minimum detectable size and coverage area will be derived and used to compare the task-based and search-based methods. These four performance metrics will be described in Chapter III, Methodology.

Justification

Air Force Space Command (AFSPC) needs improved detecting and tracking of objects in space to guard against increasing threats: “The US must sustain the ability to attribute malicious or irresponsible actions that jeopardize the viability of space for all” (JP 3-14, 2018). The GEODSS system provides almost complete coverage of the GEO belt and delivers close to 80% of all GEO observations (Bates, n.d.). In support of options for the GEODSS program office, this research investigates if they can affordably improve their telescope-network performance by changing their current task-based operating approach. With task-based surveillance, only the targets on the list are imaged/observed at regular intervals. In an interview with the GEODSS personnel, the main concern identified was areas of the sky that never get observed. A search-based approach may provide that additional coverage without significantly degrading the current performance.

Assumptions/Scope

This research will focus on modeling a ground-based telescope network, similar to GEODSS and will not include the entire SSN. The SSN consists of space-based telescopes, ground-based telescopes and ground-based radars that detect and track space objects. The model developed herein, will only include the GEO belt region when evaluating the performance for the current task-based space surveillance and the proposed survey/search-based space surveillance. The model architecture will only include GEODSS-sized ground telescopes and 813 known objects in the GEO belt (retrieved from spacetrack.org in 2016). The performance evaluation results for the

scenario studied are assumed to be representative of how the two approaches would perform under realistic conditions.

GEODSS is a set of three sites with three telescopes each. One site is located on White Sands Missile Range near Socorro New Mexico, one site is on Mount Haleakala, Maui HI, and one site is on the island of Diego Garcia.

Methodology

The methodology herein follows a similar process as Stern and Wachtel (2017) of creating a model, using AGI's Systems Tool Kit (STK) to generate data, and then using Python to evaluate the model performance. Performance will be measured by calculating the minimum detectable size, detection rate, coverage area, and latency. A baseline model will be created to emulate the current task-based operations of the GEODSS system. The baseline performance will then be compared to the search-based performance.

Thesis Preview

Chapter II provides an overview of the importance of GEO SSA and describes previous studies conducted that are similar in nature to a nightly GEO belt search. Chapter III details the methodology used herein. It explains the task-based model, how the search-based model was created and explains the changes that were made for the evaluation criteria used for the side by side comparison. Chapter IV provides the performance results of the two space surveillance approaches and compares their performance. Chapter V presents the conclusions and recommendations as well as possible future work and improvements.

II. Literature Review

Chapter Overview

This chapter provides context on the importance of SSA, and background on how the Department of Defense (DoD) currently provides GEO SSA. Previous research that used Model Based Systems Engineering (MBSE) and Modelling and Simulation (M&S) is reviewed and also includes implemented GEO belt surveys that have been accomplished. First, it presents the DoD's GEO SSA problem, and then discusses how recent research has used MBSE and M&S to produce solutions to improve GEO SSA. Lastly, it documents recent GEO belt surveys that were conducted in the last 15 years to show examples of how a survey strategy could be applied to this thesis.

Space Situational Awareness

Joint Publication (JP) 3-14, Space Operations, defines SSA as, "the requisite current and predictive knowledge of the space environment and the operational environment upon which space operations depend as well as all factors, activities, and events of friendly and adversary space forces across the spectrum of conflict" (JP 3-14, 2018). In other words, the US needs to know where every object in space is at all times whether it is a friend, enemy or piece of debris. SSA is Space Battle Management similar to that of the air domain but instead of controlling air traffic, space traffic is monitored and controlled. Having good SSA is the first step in successful and safe operations in space. Gen John Hyten, Commander of US Strategic Command, said in a 22 June 2018 House Armed Services Committee hearing, "As the commander responsible for defending the nation in that domain, I have to look at [Russian and Chinese] capabilities

as real threats and that means I have to develop counters to those threats, which is why the first thing I have to have, just like in any other domain, is that exquisite situational awareness of what is happening in that domain so that I can respond quickly enough" (Pomerleau, n.d.). The Russian satellite Olymp is an example of a possible threat that is increasing in space. Olymp was launched in September of 2014 and seven months later it maneuvered to a spot between Intelsat 7 and Intelsat 901 which are located a half degree of longitude from each other in GEO. A few months later it maneuvered again and settled next to another Intelsat, this time only a tenth of a degree away (Gruss, n.d.). The US is concerned that these types of potential threats in space are on the rise. The US Intelligence Community Worldwide Threat Assessment states, "Of particular concern, Russia and China continue to launch 'experimental' satellites that conduct sophisticated on-orbit activities, at least some of which are intended to advance counterspace capabilities. Some technologies with peaceful applications—such as satellite inspection, refueling, and repair can also be used against adversary spacecraft" (Coats, 2018). To be able to detect the increasing number of maneuvering satellites, the US needs to improve their SSA, whether it be through increasing the number of sensors or changing the method of how SSA is accomplished. Although detecting all satellite movements is a growing concern, it is not the only threat to space operations that is on the rise.

SSA is getting more difficult every year due to the increasing number of new satellites being launched. There has been roughly a 90 percent increase in the number of satellites in Low Earth Orbit (LEO) since 2014 with a current estimate of around 2,270, and the growth is expected to continue. Two private civilian companies alone have plans to launch satellite constellations that together will put upwards of 14,000 new satellites in

orbit by the mid-2020s (Beyer & Nelson, 2018). Specifically, in the GEO orbit the increase in satellites is also occurring at a high rate. From 2000 to 2009, the number of spacecraft added to the GEO orbit exceeded the number being removed at a rate of two to one. Removal of spacecraft from the GEO orbit after the end of a mission life has been recommended for decades, but the number of large objects in GEO continues to grow (Johnson, 2010). According to spacetrack.org, there are currently 851 Two Line Element Sets (TLES) for known objects in the GEO belt that have received an update within the past 30 days as of 24 July 2018. In addition to the increasing number of new satellites being launched, the amount of space debris is also increasing in the GEO belt. NASA estimates that there are approximately 3,250 GEO objects 10 cm or larger as shown in Figure 1, derived from NASA Space Debris Quarterly. The uncatalogued debris

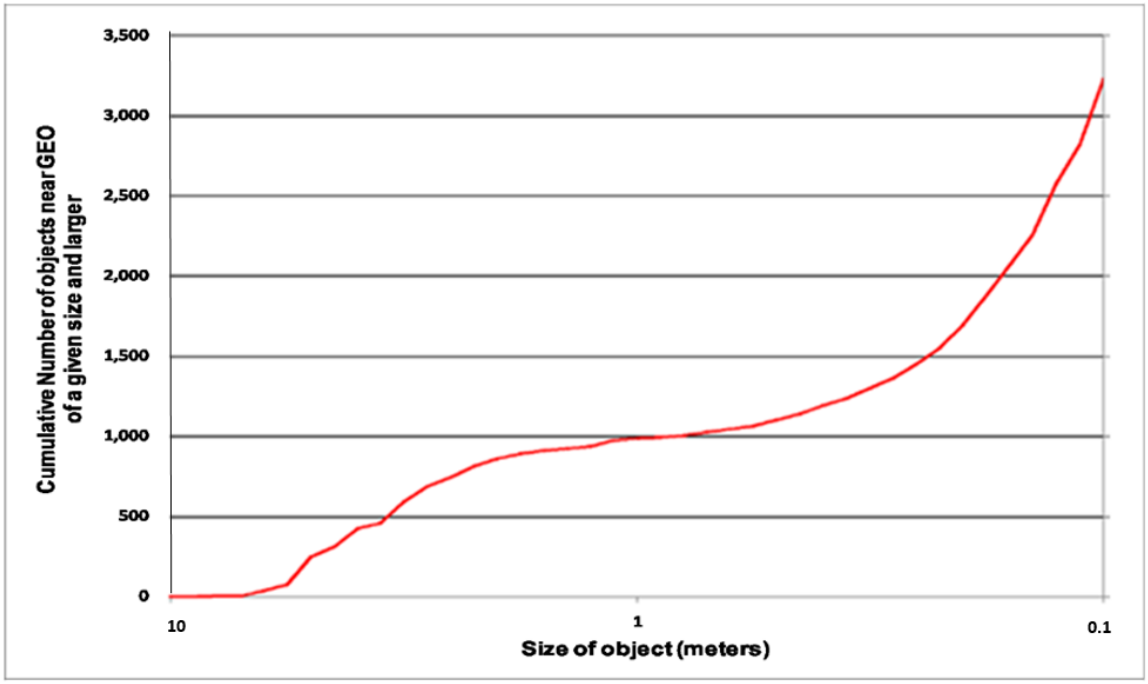

Figure 1: NASA Assessment of the Near-GEO Satellite Population (Johnson, 2010)

population near GEO exceeds that of the known satellite population (Johnson, 2010). The US Air Force created and maintains the satellite catalog that contains over 23,000 man-made earth-orbiting objects, also known as Resident Space Objects (RSOs). The satellite catalog is a database that contains the most up-to-date orbital parameters of tracked objects in space. Maintaining this catalog for the ever growing RSO population has become more difficult over the years for the Space Surveillance Network (SSN).

Space Surveillance Network

The Air Force maintains the space catalog through a global network of 29 radars, ground-based optical telescopes and space-based optical telescopes known as the SSN (USSTRATCOM, 2010). The GEO belt portion of the space catalog is maintained primarily by the GEODSS telescopes. The Eglin phased array radar, the Globus II X-Band dish radar, the Space Based Space Surveillance (SBSS) system, and the new Geosynchronous Space Situational Awareness Program (GSSAP) satellites also contribute to the maintenance of the GEO belt region of the space catalog. These systems feed observed satellite position data to the JSpOC where it is processed, and updates to the satellite catalog are made. Below are descriptions for the systems that provide observations in the GEO belt.

GEODSS

GEODSS is a set of three sites, Detachment 1 located near Socorro, NM; Detachment 2 on Diego Garcia in the Indian Ocean; and Detachment 3 on top of Mount Heleakala on Maui, HI. Each site consists of three one-meter aperture telescopes with a two square degree FOV. GEODSS has been in operation since the early 1980s and can

see objects as faint as 16 visual magnitude.[3] As with any ground optical system, it is limited by lighting conditions, cloud cover, and local weather (AFSPC, 2017b).

Eglin Radar AN/FPS-85

The Eglin phased array radar is the most powerful radar in the world and is the only radar capable of tracking objects in the GEO orbit. It can track objects in LEO that are the size of a baseball and objects in GEO that are about the size of a basketball. The radar has been in operation since 1969 and is located on Eglin AFB in Florida (Stuckey, 2011).

Globus II

Globus II is an X-Band radar that is located at Vardo Norway. It is operated by Norwegian personnel but was developed by the US. Globus II uses narrowband, wideband and other specialized waveforms which gives it the highest resolution capabilities of all existing USAF radars (Colarco, n.d.).

SBSS

SBSS is a space-based observer satellite that is in a sun synchronous orbit at an altitude of 630 km. The orbit gives the satellite almost complete coverage of the GEO belt in a 24-hour period. The satellite has an optical telescope with a 30 cm aperture, a 2 degrees by 4 degrees FOV, and a sensitivity of being able to view targets as faint as 16.5 visual magnitude (Ackermann, Kiziah, Zimmer, McGraw, & Cox, 2015).

GSSAP

GSSAP is a set of four satellites that are in a near GEO orbit that take observations of RSOs in the GEO belt. The first two were launched in July of 2014 and

[3] Visual Magnitude is a brightness measurement number as seen by an observer from the Earth.

two additional satellites were launched in August of 2016. From their near GEO orbit, these observer satellites perform Rendezvous and Proximity Operations (RPO) to get unobstructed views at much closer ranges than any other sensor in the network (AFSPC, 2017).

Despite the global placement of sensors and the power of these systems to peer into the GEO belt, there are several difficulties that prevent persistent SSA, which is the ability to see every object at all times. The lack of persistent observations on objects can lead to objects being "lost" and require a lot of effort to find again. A "lost" object means it could not be observed with a clear line of sight while attempting to make a subsequent observation at a later time, which could be hours or days after the last observation. It can also give adversary satellites the opportunity for unnoticed maneuvering and un-attributable damage. The following are impediments of observing objects in GEO (Ackermann et al., 2015):

1. No matter where sensors are placed, either on the ground or in space, there will always be a time when objects will be un-viewable. Ground telescopes are limited to night time viewing while space-based sensor views are blocked by the Earth and are unable to see the target when it is between the sensor and the Sun.
2. Objects in GEO are hard to see because the view distance is around 35,000 km or more. There are many objects in GEO that are just simply too small to be detected by any available sensors.

3. The optimal placement of ground-based telescopes is at high altitudes and as close to the equator as possible. Optimal locations are often remote and difficult places to build and maintain sites.
4. The GEO belt is a vast region of space to keep track of at all times. Taking faster observations to cover more targets sacrifices the ability to detect smaller objects. Sky coverage is also difficult because of the tasked base process of observation the SSN uses.

Bernstein's (2013) paper on the SSN tasking process gives a good overview of how the space catalog is maintained. The JSpOC sends taskings to these systems to take observations on a daily basis. The sites and systems receive the taskings and attempt to collect the observations for which they are tasked. To be clear, tasking and scheduling are separate activities. The scheduling of when to take observations of any particular object is determined by each site or system. In the case of GEODSS, scheduling of the observations depend on if there is a clear line of site between the telescope and the object of interest. If the object is unable to be observed at a particular time the scheduler will skip over the tasking and try again at a later time. Successfully completed observation tasks are sent back to the JSpOC for correlation and comparison to the space catalog. All orbit determination and classification is done at the JSpOC. Observations that match to a known object in the space catalog are called "Correlated Tracks" (CTs) while observations that do not match the catalog are called "Uncorrelated Tracks" (UCTs). Sites are restricted to observing objects that are on the task list sent from the JSpOC (Bernstein, 2013). On occasion, small area searches are performed when an expected object is not detected in the first FOV. In this case the sensor will take observations

behind or in front of the expected path of the object's orbit till something is detected or a time or angular threshold is reached. However, no full sky searches or scans are ever done.

Relevant Research

The goal of this research is to show how doing a nightly scan of the sky impacts performance of ground-based telescopes by using dynamic M&S. The International Council on Systems Engineering (INCOSE) defines MBSE as "a formalized application of modeling to support system requirements, design, analysis, verification and validation, beginning in the conceptual design phase and continuing throughout development and later life cycle phases" (Friedenthal, Griego & Sampson, 2007). A simpler definition of MBSE is "a way of modeling requirements, design, analysis, and verification activities as a cost-effective way to explore system characteristics" ("SAFe Scaled Agile," 2017). MBSE differs from conventional simulation in that there first exists a descriptive model of the system architecture often, though not always, using SysML. This thesis intends to model the performance of a GEODSS like system in task mode and search mode to explore differences in the system's performance. MBSE and M&S allows researchers to gain valuable insights without having to take time away from operational assets or setting up expensive test scenarios. It also can help provide answers when there has been little to no previous research done on the topic. MBSE and M&S methodologies can help assess preliminary design trade spaces for performance and value comparisons. Several previous researchers have used MBSE and M&S techniques to come up with possible solutions to complex Systems Engineering (SE) problems.

An excellent example of M&S techniques is in the paper by Choi in the *Journal of Astronomy and Space Science*. The authors concluded "A strategy is needed for a regional survey of geosynchronous orbits (GSOs) to monitor known space objects and detect uncatalogued space objects" (Choi et al., 2015). STK and TLE's from the JSpOC were used to simulate the orbits of 287 RSOs in view of a telescope site located in Daejoeon, South Korea. The study simulated four survey observation strategies; 5-second exposures with the 1º x 1º FOV, 5-second exposures with 2º x 2º FOV, 2-second exposures with a 1º x 1º FOV and 2-second exposures with a 2º x 2º FOV. A scanning motion in the local reference frame is used to look at the GEO belt region that is viewable from the Daejoeon site. Figure 2 shows the graph of a sample scan pattern used with a 2º x 2º FOV. The scan first moves vertically in the elevation direction then moves over to the next column of elevation going 17 intervals deep. Intervals are simply the width/height of the FOV used as indicated by the green and blue boxes in Figure 2. Green indicates a 17 interval 2º x 2º FOV scan while the blue is a single 2º x 2º FOV scan. The study found the FOV was the most important variable in obtaining high detection rates. The 5-second exposures with the 2º x 2º FOV showed the best results with detection rates of 90% and 95% for non-operational and operational RSOs respectively. A smaller observation duration increased detection rates by only 2%–3% but the longer exposure allowed for better Signal to Noise Ratio (SNR), therefore the longer exposure was chosen (Choi et al., 2015).

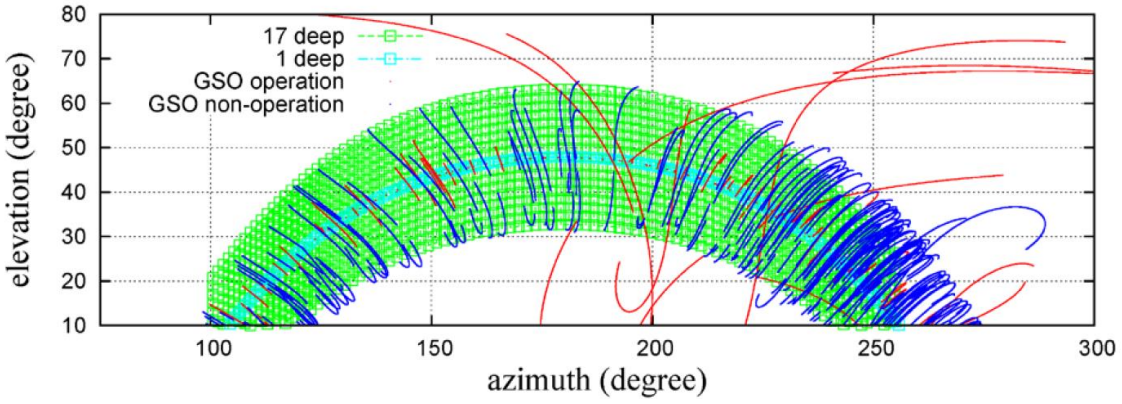

Figure 2: Scan Pattern of the Analysis of Simulated Optical GSO Survey Observation Paper (Jin Choi 2015)

A second example of modeling GEO search was done by Flohrer in the *Advances in Space Research* journal. The study was on a possible space surveillance telescope network for the European Space Agency that was modeled to assess performance against needed requirements (Flohrer, Schildknecht, Musci, & Stöveken, 2005). The model was made up of 4 telescope stations placed around the world and a catalog of 793 objects in GEO were used in the simulation. The model assumed a "stripe scan" survey strategy that picked a right ascension to follow for 24 hours and covered a declination of +/- 17º as shown in Figure 3. Using this scan strategy every object with an inclination less than 17º will pass through the FOV in a 24-hour period. Due to the limited FOV of the simulated telescope, the scan will complete a full "strip" once every 15 days. The Program for Radar and Optical Observation Forecasting (PROOF) (Krag et al., 2000) tool was used to estimate the minimum detectable size and coverage. With a 1 meter telescope in survey mode, objects could be seen down to 25 centimeters in diameter and detection rates were 89.8% and 94.7% for 8-hour and 12-hour observations per night respectively. The

authors concluded that a space surveillance system for GEO needs to have three to four sites and each must be able have both dedicated survey and dedicated tasking telescopes (Flohrer et al., 2005).

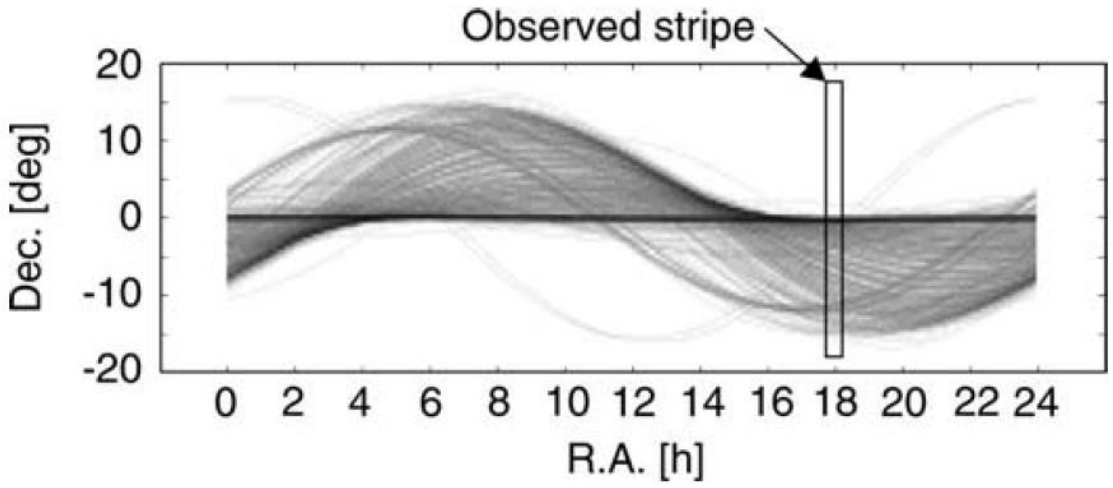

Figure 3: Scan Pattern for Performance Estimation

for GEO Space Surveillance Article (Flohrer et al., 2005)

Similarly the work by Flohrer, Schildknecht, & Musci in *Advances in Space Research*, states "It is most advisable to combine survey and tasking strategy" and " 'survey only' strategy may not always be used for GEO space surveillance due to the FOV limitations. The correct detection of maneuvers cannot be guaranteed" (Flohrer, Schildknecht, & Musci, 2008). The authors confirm that GEO should be covered by the same "stripe-scanning" approach as the 2005 "Performance estimation for GEO space surveillance" paper. The study also confirmed Choi's conclusion on wider FOVs, stating "a wide FOV survey sensor, which covers the entire survey band, would likely be the most efficient strategy" (Flohrer et al., 2008).

A third example of the use of M&S to solve a complex SE problem is the paper on the Defense Weather System Follow-on (WSF) system (Thompson, Colombi, Black, & Ayres, 2015). This paper addresses the problem of whether to use a multi-orbit disaggregated space system or a large multi-function spacecraft as a solution for the WSF. Very little research literature existed on the trades between the use of a large number of small satellites and the traditional large satellite system deployment. The paper shows that through modeling and simulation and the use of an optimization methodology they were able to identify, assess, and compare different space-based weather system architectures. In the end the model converged on a disaggregated small satellite system as the optimal solution for the WSF based on evaluation of lifecycle cost, sensor performance, and probability of coverage (Thompson et al., 2015).

Stern and Wachtel (2017) used an MBSE and M&S approach to find an optimal SSN architecture, made up of ground-based telescopes and space-based observers in different orbit regimes which had the best performance based on the smallest viewable object size and the latency and the cost to build such an architecture. They used STK and Python to model and simulate 813 GEO RSOs using TLEs, retrieved from spacetrack.org, and developed a scheduler in Python to emulate how the SSN tasks its ground telescopes, and space-based observers. STK was used to generate access reports with azimuth, elevation, range, and phase angle values. Then Python was used to process the STK reports and calculate the size, latency and cost values for the various surveillance architectures (Stern & Wachtel, 2017). Felten (2018) also used the same method but expanded the possible SSN architectures in the trade space, allowing Geosynchronous Polar Orbits (GPO). Both demonstrated a way to use MBSE to come up

with solutions to a complex systems engineering problem that would take far too long and be too expensive to implement and test in the real world.

Lastly, the Wide Eye-Narrow Eye Space Simulation for Situational Awareness (WENESSA) is developing a M&S capability that is using the Tasking of Autonomous Sensors in a Multiple Application Network (TASMAN) as a simulation framework. TASMAN is a physics-based SSA network simulation environment that includes models of the Space Surveillance Telescope (SST), GEODSS, and the Dynamic Optical Telescope System (DOTS). DOTS is a set of smaller diameter telescopes and one large diameter telescope at the Maui Space Surveillance Site on Maui HI. DOTS looks for anomalies with the smaller diameter telescope and follows up with a larger diameter telescope for detailed observation when needed. The goal of WENESSA is to build an M&S capability that can evaluate performance of DOTS like systems at multiple sites. A stated goal is to make it a modular and developed in an open source code environment that will not need knowledge on the complexities of the code allowing for quick turn studies of different space surveillance architectures (Alba et al., 2017).

This thesis intends to use MBSE to assess the performance of a tasked-based verses a search-based method of space surveillance. Further discussion on the methodology and the similarities and differences between this thesis and previous work will be presented in Chapter III. MBSE can be effective at refining a preliminary solution. It can quickly give model tested solutions in a cost effective manner but when compared to real-world implementation and testing of a solution, the model can vary from reality. As George E.P. Box said, “All models are wrong, but some are useful” (“SAFe Scaled Agile,” 2017).

Implemented GEO Surveying

The search-based method of space surveillance is basically a nightly survey of a portion of the sky. Over the past couple of decades there have been several surveys of the GEO belt performed to characterize debris fields, detect operational satellites, assess the GEO population and track the evolution of fragment clouds. Specific surveys discussed in this thesis were performed by the Russian International Scientific Optical Network (ISON), National Air and Space Agency (NASA), and the Air Force Research Laboratory (AFRL). This section will discuss the methods used to perform these surveys and some of the results.

The goal of the NASA GEO survey was to help characterize the GEO debris environment. NASA used the Michigan Orbital Debris Survey Telescope (MODEST) located in Chile to perform the survey over a period of three years. MODEST is a 0.61-m aperture telescope with a 1.3 by 1.3 degree FOV that can see objects fainter than 18 visual magnitude assuming a signal to noise ratio of 10 (Abercrombly, Seitzer, Barker, Cowardin, & Matney, 2010). The survey took place over 36 nights in 2007, 43 nights in 2008 and 43 nights in 2009. The survey was limited to 15 degrees above and below the equatorial plane since GEO RSOs can oscillate inclinations from +/- 15 degrees every 50 years. Each night MODEST would be pointed at a right ascension and declination that was closest to the best solar phase angle and stared at that point through the night. The survey found that there were 3,143 objects in GEO, in the MODEST's viewable portion of GEO, with about 25% of them being "Uncorrelated Tracks" UCTs. The UCT percentage went up to 40% when only objects with inclinations greater than 1 degree

were considered. Figure 4 shows the inclination vs. the Right Ascension (RA) overlaid with “Correlated Tracks” CTs and UCTs (Abercrombly et al., 2010).

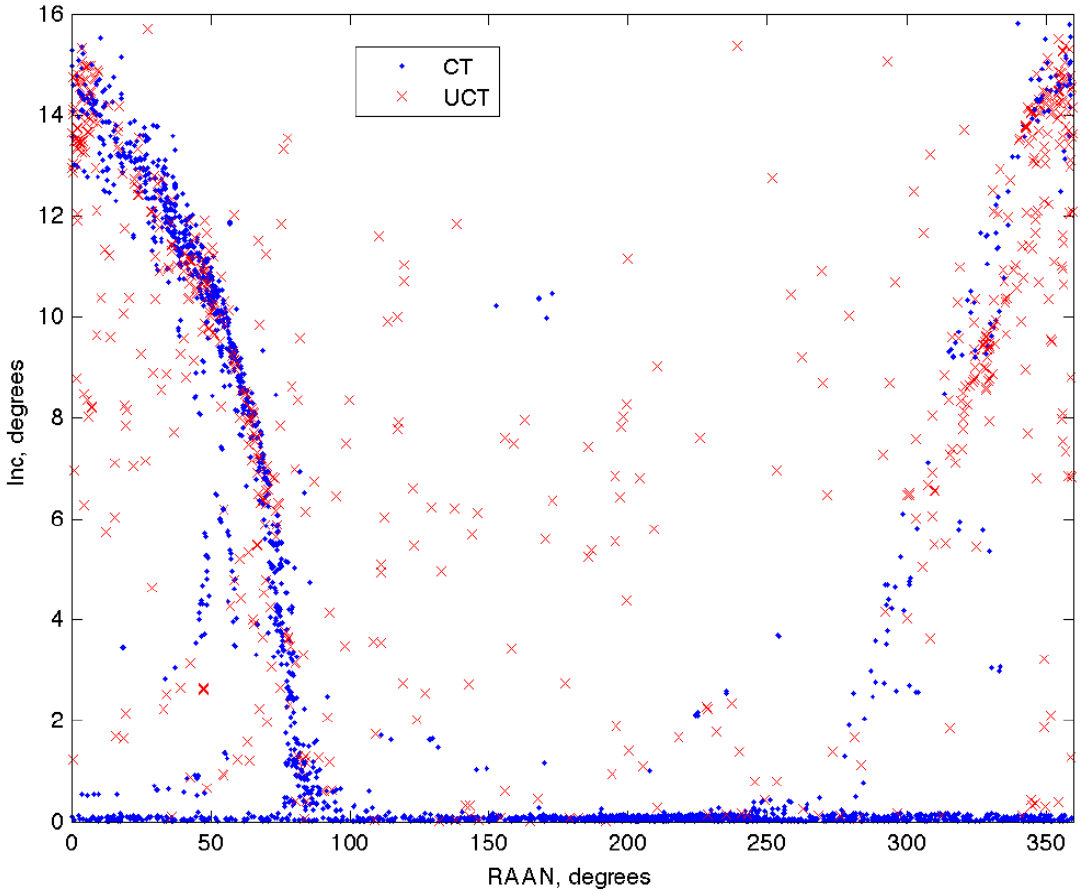

Figure 4: RAAN vs. Inclination for CTs and UCTs over 3 Years (Abercrombly et al., 2010)

The goal of the ISON survey was to find the distribution of GEO objects in the protected region. The protected region is similar to the NASA survey with inclination boundaries of 15 degrees above and below the equatorial plane and orbit radius of ±200 km of true GEO altitude (Agapov, Molotov, & Khutorovsky, 2009). The ISON survey used 32 telescopes dispersed across Russia with one telescope in South America. The telescopes had apertures between 0.2 and 2.6 meters and FOVs ranging from 1 degree to

24 degrees (Molotov et al., 2009). The report "Analysis of Situation in GEO Protected Region" covers survey results from its beginning in 2005 to 2009. The significant finding from the paper is the ISON started to implement a survey strategy in 2009 where as before it used an "object-to-object rounds" strategy. From 2008 to 2009 the number of orbits maintained on a regular basis increased from 1,243 to 1,441, and UCTs dropped from 2.8% to less than 1% according to the paper (Agapov et al., 2009).

The goal of the AFRL study was to survey the population of active and inactive objects and to validate the results of the 2006 European Space Agency (ESA) survey done in 2006. AFRL used the Panoramic Survey Telescope and Rapid Response System (Bolden, Sydney, & Kervin, 2011), also known as PAN-STARRS, to conduct the survey over two nights. The survey method was similar NASA's method of scanning; the telescope was pointed at a single RA and moved up and down declinations as it scanned across the sky from east to west. The PS1 is a 1.8m aperture telescope with a sensitivity of 21 visual magnitude and a 7 square degrees FOV. The GEO survey took place in 2010 and was compared to ESA survey done in 2006 as shown in Figure 5.

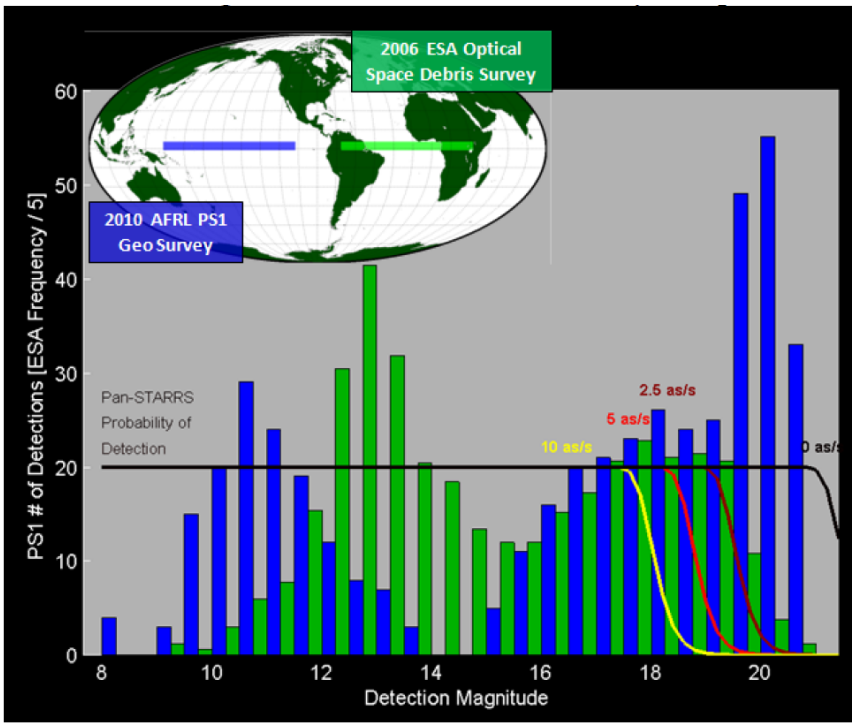

Figure 5: AFRL and ESA GEO Survey Comparison (Bolden et al., 2011)

The results of the surveys show that there are two distinct populations of objects across the visual magnitude range. One population is between 10 and 15 visual magnitude, and a second is between 15 and 20. It is theorized that brighter objects that have visual magnitudes less than 15 are mostly active or inactive satellites and objects fainter than 15 are mostly debris (Bolden et al., 2011).

The results of these implemented surveys show that there are more objects in GEO than what is currently being tracked and characterizes the size distributions in GEO. As previously mentioned, there are approximately 851 TLEs for known objects in the GEO belt. This shows that there are many objects that are not being seen with a task-based surveillance method. These surveys also show search constraints, such as debris oscillating at +/- 15º inclination, can narrow the necessary search area and make searches

more efficient. This thesis uses these survey results to help constrain the search method presented in Chapter III.

Summary

This literature review covered the importance of SSA, how the SSN works, and the difficulties of GEO SSA. It then reviewed relevant research and showed how MBSE can be used to come up with solutions to complex engineering problems. Finally the literature review discussed three GEO belt surveys that were implemented with a variety of telescopes and search methods. Although previous research and implemented surveys show that there are some possible techniques for surveying and interesting trends in distributions of satellites in GEO, they do not go much beyond those results. The previous research and surveys do not show a good side by side comparison of search-based vs. task-based space surveillance. Thus, there needs to be research that utilizes a survey strategy for orbit maintenance and a way to compare it to the current task-based approach.

III. Methodology

Chapter Overview

The purpose of this chapter is to explain the methods used to find performance values of the task-based and search-based space surveillance techniques. The performance metrics are smallest detectable size, latency, detection rate, and coverage area. This chapter will also discuss the major phases of the thesis which are data generation, modeling the task-based and search-based scheduler, and evaluation development. The output of the model will be a set of performance metrics that can then be used to compare and evaluate the two surveillance techniques.

Theory

As discussed in Chapter I, the space domain and in particular the GEO belt, is getting more congested, contested and competitive each year. To support options for the GEODSS program office, this thesis will estimate system performance if operated with a strictly search-based approach. The expectation is that a nightly scanning of the sky will improve SSA performance and cover gaps of the sky that would never be viewed with the current baseline task list surveillance technique. Performance for this thesis will be measured by smallest detectable size, latency, detection rate, and coverage area. Early hypotheses are that the task-based baseline will outperform search in latency and detection rate while the search-based will perform better in detectable size and coverage area.

Materials and Equipment

STK

The Analytical Graphics Incorporated (AGI) Systems Took Kit (STK) was used to model the scenario and generate the access data for each ground site. STK is a modeling tool that simulates satellite motion and produces various reports such as phase angles, zenith angles, azimuth and elevation angles, and range that can later be analyzed. Model scenarios were set up and run via AGI's "connect" commands using Python.

Python

Python is a commonly used high level programming language free to the public. Through the use of scripts, "connect" commands and a TCP socket, Python was used to command STK to generate the scenario and report files for the data generation phase. It was also used to model the search scheduler and evaluate the performance metrics. Through the use of loops and connect commands, Python is able to generate and batch process data at a high rate allowing for fast results.

Previous Thesis Code

Previous thesis code was used and modified to fit the purpose of this thesis. The data generation, scheduler, and evaluation code used in the Stern and Wachtel (2017) thesis was used as a baseline. Some assumptions and limitations that were built into the code were also carried over into this thesis. These assumptions and limitations include solar and lunar exclusion angles for the telescopes and the 30 second greedy scheduler which is assumed to emulate the real-world task-based surveillance. Also data generation scenarios were limited to a single 24-hour period but could be run on different dates as desired.

High Level Approach

In order to compare the task-based vs. search-based surveillance techniques the four performance metrics (smallest detectable size, latency, detection rate, and coverage area) must be determined for each. The data generation and scheduler code used in the Stern and Wachtel (2017) thesis is used to model the baseline task-based technique while the search scheduler is newly developed. The task-based and search-based scheduler then feed into the evaluator that outputs metric values. The evaluator uses the Stern and Wachtel (2017) code to calculate the latency metric values. New code was developed to model and calculate the smallest detectable size, coverage area, and detection rate metrics for the task and search methods.

In MBSE the Systems Modeling Language (SysML) is "a graphical modeling language that enables you to visualize and communicate the aspects of a system's design: structure, behavior, requirements, and parametrics" (Delligatti, 2014). Using SysML is a good way to graphically show the high-level methodology. Figure 6 is a block definition diagram (BDD) that describes the items that make up a ground-based GEO surveillance system. Figure 7 is an activity diagram describing the control flow within the model created.

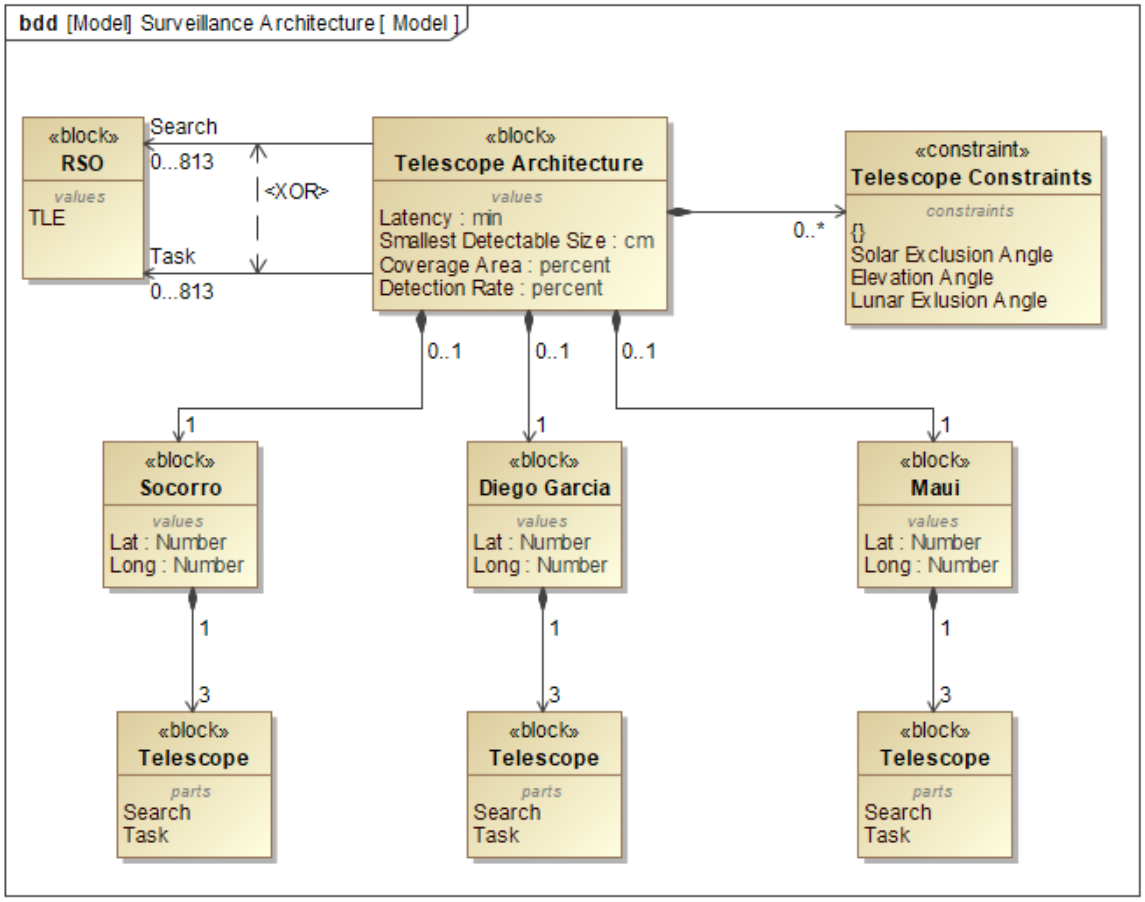

Figure 6: Block Definition Diagram of the Model Architecture

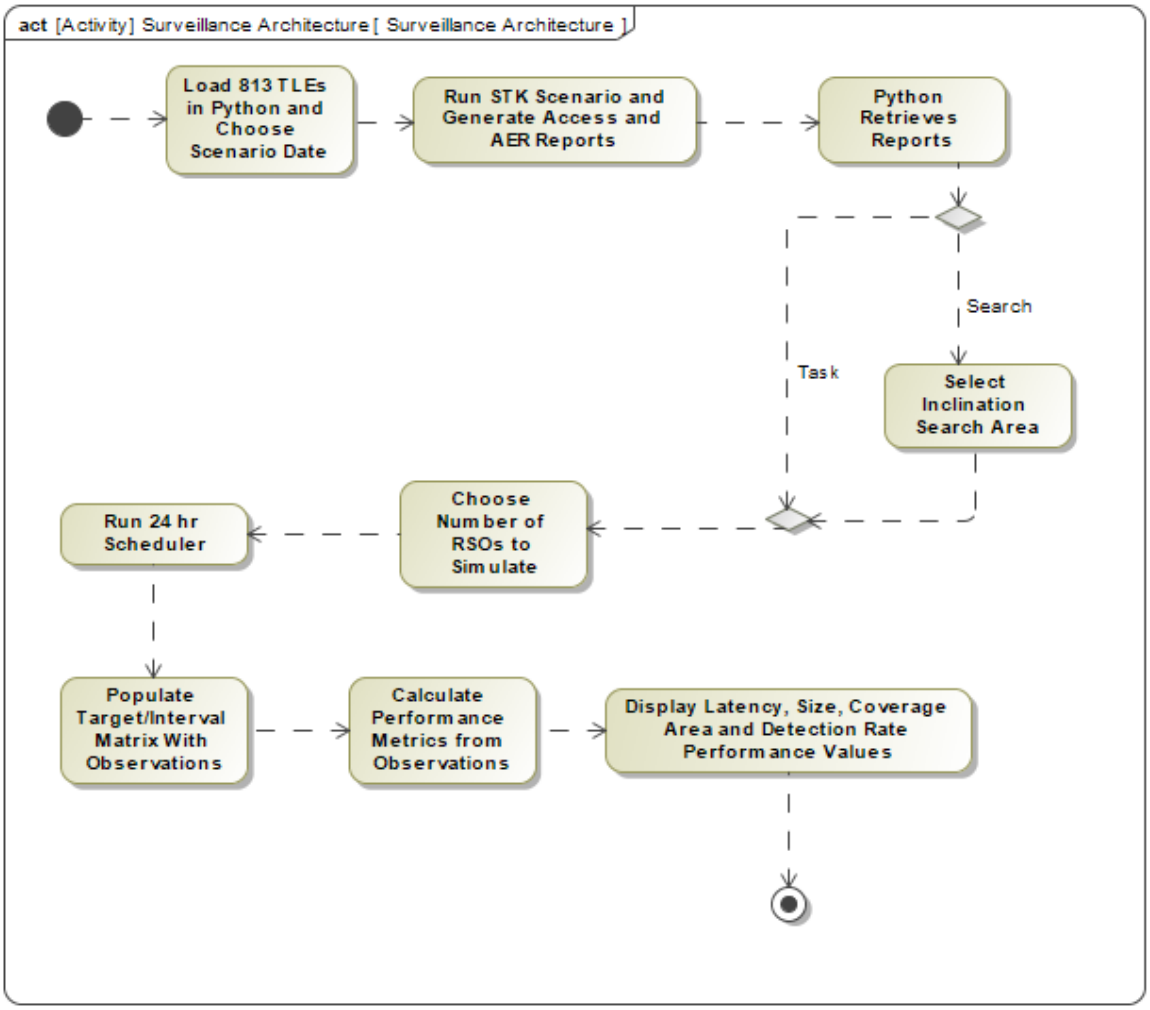

Figure 7: Activity Diagram of Model

Data Generation

The first step in assessing performance is to create the scenario and generate the data needed for the scheduler. Using Python and connect commands with STK, the scenario was set up for a 24-hour period on the summer solstice, fall equinox and the winter solstice in 2018 with time steps of 30 seconds. The 21 Jun, 22 Sep and 21 Dec dates were chosen to get results for the varying lighting conditions during the year. Ground-based telescopes were placed at the three GEODSS locations of Socorro, NM;

Maui, HI; and Diego Garcia. All telescopes were given solar exclusion angles of 40º, lunar exclusion angles of 10º, minimum elevation angles of 15º, and were limited to operating in umbra. Stern and Wachtel (2017) and Felten (2018) thesis used similar values except they used 20º for minimum elevation. In "Analysis of a Simulated Optical GSO Survey," 10º elevation was used (Choi et al., 2015). A 15º minimum elevation was used in this thesis to more closely model existing operations.

Simulated RSOs were generated using the 813 GEO TLEs obtained from spacetrack.org. All RSOs were assigned the J2 perturbation model and were assumed to only be visible to the ground-stations when they were in direct sunlight. This was consistent with the Stern and Wachtel and Felten methods.

Once all RSO and ground stations are created, STK runs the scenario and generates lunar & solar phase angles, lunar and target zenith angles, access reports, azimuth/elevation/range reports, and moon phase reports for every ground-station to RSO pair. These reports are then used in modeling the scheduler for both the task-based and search-based schedulers.

Since all data generated is in the local azimuth and elevation reference frame, a transformation formula was coded to convert from a local frame to a global latitude/longitude frame for each of the ground station locations. Transformation is necessary to figure out the telescope viewing limits to constrain the search pattern in the global reference frame. This longitudinal range is constrained by the minimum 15º elevation angle and the lowest altitude of the GEO belt, approximately 35,595km, as viewed from the location of the ground station. As an example, due to Diego Garcia's location near the equator it is able to see GEO RSOs in the entire range of +/- 16.97º

declination from 10ºW to 135ºW longitude. Thus the search area for Diego Garcia telescopes is constrained to this coordinate box. The code for this reference transformation is located in Appendix A.

Scheduler

Baseline Task-Based Scheduler

A baseline model of current task-based operations is needed to create a comparison. The scheduler modeled by Stern and Wachtel was used to simulate the current task-based operations. The scheduler assumes it takes 30 seconds to take a 3-observation tracklet and then slew to the next RSO. A typical single observation exposure is 2–5 seconds. The Michigan Orbital Debris Survey used 5 second for exposures and the "Analysis of a Simulated Optical GSO Survey" technical paper used 2 seconds and 5 seconds for their models (Abercrombly et al., 2010; Choi et al., 2015). Based on this, 30 seconds is a sufficient amount of time to simulate three 5-second exposures and slewing to the next RSO location. Full details on how the scheduler is modeled can be found in the Stern and Wachtel (2017) thesis, pp 57–58 (Stern & Wachtel, 2017). The scheduler prioritizes RSOs by always observing the RSO, in its field-of-regard that has the largest time gap from its last observation. An observation is only credited on the RSO that had the highest time gap and not for any other RSO that may have been in the same FOV at the time. The scheduler produces a matrix of 1s and 0s for each 30 second interval indicating whether the ground station has a line-of-site for each RSO. This matrix then feeds into the evaluation phase. The model's goal is to emulate the typical operations of completing the nightly observation task list sent from the JSpOC. The task-based scheduler is run on 21 Jun, 22 Sep, and 21 Dec.

Search-Based Scheduler

The search-based scheduler was developed assuming the same 30 second allotment to complete three 5 second exposures and required slewing operations. The scheduler simulates a scan of the GEO belt +/- 16.97º above and below the equator similar to the +/- 17º used by Flohrer (2005). To cover at least +/- 15º of inclination, eight FOV intervals had to be used which expanded the search area to +/- 16.97º. Six FOV intervals would only cover +/- 12.73º. The scan starts in the eastern sky and works its way west, moving downward and then eastward after a completed vertical scan, staying within the +/-16.97º boundary, similar to the Choi paper. Each 30 seconds the telescopes slew to the next FOV and perform its three 5 second exposures. Each FOV has an area of 1.4º x 4.2º to simulate a coordinated effort of 3 telescopes at the ground station moving in unison. GEODSS telescopes have an advertised FOV of 2º square and each site has 3 telescopes (Bruck & Copley, 2014). Figure 8 shows the concept of the scanning motion with each rectangle representing a 30 second observation. As the telescopes scan the sky, any RSO that is within the FOV at the given interval is credited with being observed.

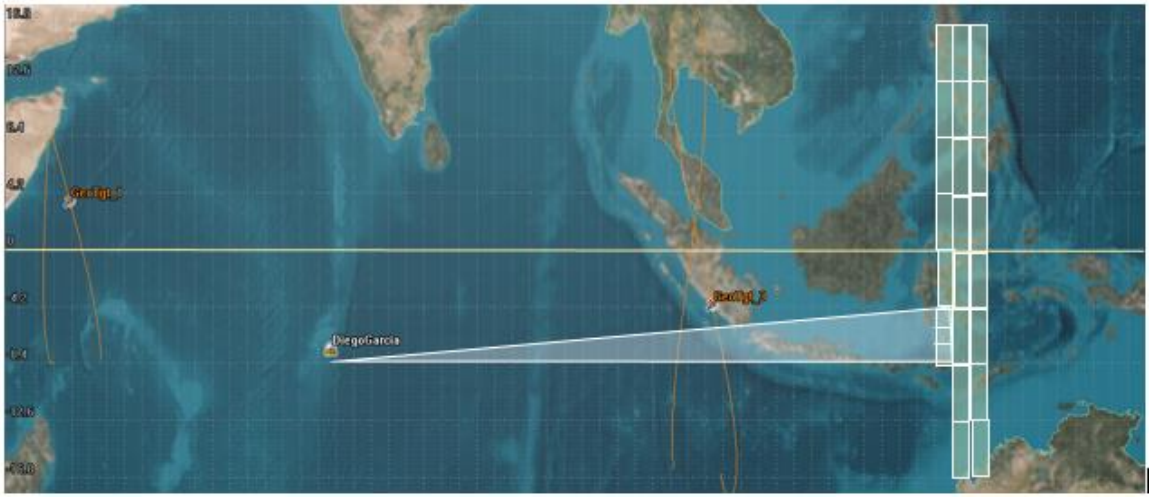

Figure 8: Scanning Pattern of the Search-Based Scheduler

This scheduler produces a similar matrix of 1s and 0s as the task-based scheduler, indicating access at each interval for the ground station/RSO pair. This matrix also feeds into the evaluation phase. In addition to +/-16.97º, smaller searches of +/-12.73º, +/-8.48º, +/-4.24º, and +/-2.12º were run. The smaller search areas were a function of decreasing the number of latitudinal FOV intervals. The final run turned the FOV on its side covering +/-0.71º in latitude and 4.24º in longitude. Each inclination search area was run on 21 Jun, 22 Sep and 21 Dec just like the tasking scheduler. Also, 10 different starting positions for each date and inclination search area were run. Search starting positions were equally spaced across each site's FOV. The first starting position starts in the eastern sky for each site location and then shifted west over to the next starting position. The 10 different starting positions provide more data points to make sure consistent values were being found for size, latency and detection rate. Coverage area will remain constant because it is a function of the inclination search area.

Performance Evaluator

Minimum Detectable Size

For determining minimum detectable size an assumed telescope performance of 18 visual magnitude was used instead of using an assumed SNR of 6 as used in the Stern and Wachtel (2017) and Felten (2018) theses. A visual magnitude of 18 is an approximate estimated performance of a 1-meter telescope. Equations (1–3) were used to solve for a minimum detectable size when given a visual magnitude (Cognion, 2013),

$$F_{diff}(a_o, r_{sat}, \phi) = \frac{2}{3} \cdot a_o \cdot \frac{r_{sat}^2}{\pi R^2} \cdot (\sin(\phi) + (\pi - \phi)\cos(\phi)) \quad (1)$$

$$r_{sat} = \sqrt{\frac{RCS}{\pi}} \quad (2)$$

$$m_V(\phi) = -26.74 - 2.5 \cdot \log(F_{diff}(\phi)) \quad (3)$$

where,

F_{diff} is the incident solar flux reflected by the spherical RSO

a_o is the RSO's albedo

r_{sat} is the radius of the spherical satellite

R is the range between the RSO and the ground station

ϕ is the phase angle

RCS is the cross section of the RSO in square meters

m_V is the apparent visual magnitude.

It is assumed that the RSO is a Lambertian (diffusely-reflecting) sphere when using Equations (1–3) (Cognion, 2013). An albedo of .175 was used in this thesis and is consistent with Cognion's 0.2 and Stern and Wachtel's 0.15.

Atmospheric transmission is also factored in by using Laser Environmental Effects Definition Reference (LEEDR) to create an elevation vs. transmission curve. LEEDR was used to scale the drop in maximum visual magnitude performance from 90º elevation down to 15º. For night time viewing, objects lose about half their brightness going from 90º elevation to 15º, which equates to a loss of about one visual magnitude from the maximum viewable magnitude of the sensor (Schaefer, 1986). For example in this thesis, the maximum visual magnitude of 18 is at 90º and is scaled down as elevation approaches 15º, using the LEEDR atmospheric transmission curves. LEEDR curves were generated for each location and date. See Appendix D for an example LEEDR curve graph. Equation (4) is used to calculate the reduced visual magnitude,

$$m_{V\ reduced} = 18 - (1 - \tau_{ATM}) \quad (4)$$

where,

τ_{ATM} is the atmospheric transmittance at a particular location, date and elevation angle

The reduced visual magnitude is then used to solve for the radius of the satellite using Equations (1-3). Then diameter is calculated using Equation (5).

$$D_{min} = 2 * r_{sat} \tag{5}$$

Detection Rate

The second performance metric is detection rate, which is the number of RSOs that are observed out of the possible number of RSOs in the FOV of the network in a single 24-hour period. This is expressed as a percentage. Detection rate is calculated using Equation (6),

$$DR = 100 * \frac{TO}{PT} \tag{6}$$

where,

DR is the detection rate percentage

TO is the number of unique targets observed

PT is the number of possible targets in the network FOV[4]

Coverage Area

Coverage area is the third performance metric that is used to compare the task-based and search-based surveillance techniques. Coverage area is defined as the number of square degrees that were viewed, in the global reference frame, in a 24-hour period. Coverage area for the search-based technique is simply summing the area scanned by the

[4] Network FOV is the total aggregated simulated FOV for all site locations

three ground stations. Figure 9 shows the three viewable regions of the GEO belt from each ground station location.

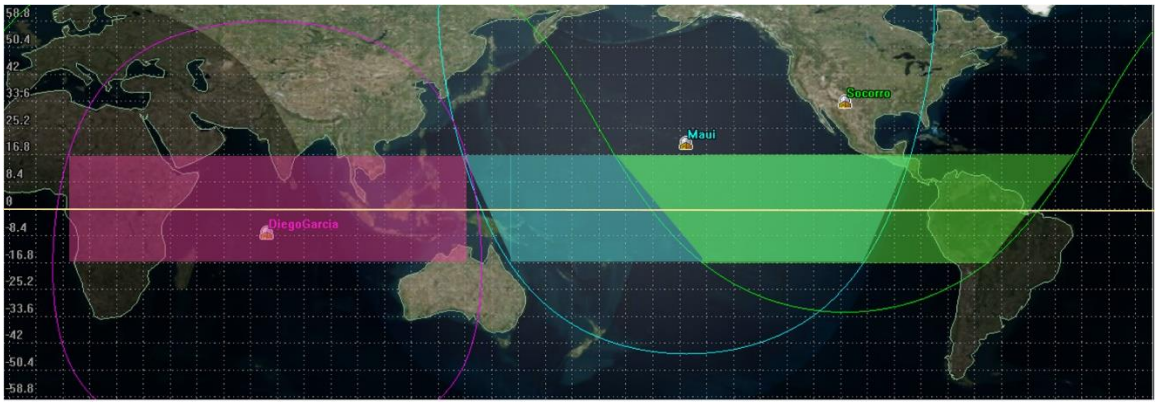

Figure 9: GEO Belt Regions Viewable from Each Modeled Location

Coverage area for the task-based approach is more difficult to calculate. To come up with a coverage area provided by the task-based approach, a grid is set up with each box representing a 1.4ºx1.4º FOV. As the task-based scheduler runs, it takes observations of individual RSOs. When the observation is taken, the RSO is located in one of the 1.4ºx1.4º grid box FOVs. The task-based scheduler then gets credit for viewing that particular grid square of coverage area. As observations are taken through the night, the grid boxes are checked off as being viewed. At the end of the 24-hour period, the total number of squares viewed is summed up to give a total coverage area viewed by the task-based scheduler. Figure 10 shows concept of the how coverage is tracked. Certain RSOs may be viewed multiple times along their orbit depending on the timing and access of the RSOs. Note that the grid is not to scale for viewing ease. Coverage area is calculated using Equation (7),

$$CA = 100 * \frac{VB}{TGB} \tag{7}$$

where,

CA is the coverage area percentage

VB is the number of 1.4ºx1.4º grid boxes viewed

TGB is the total number of 1.4ºx1.4º grid boxes within +/-16.97º of the equator

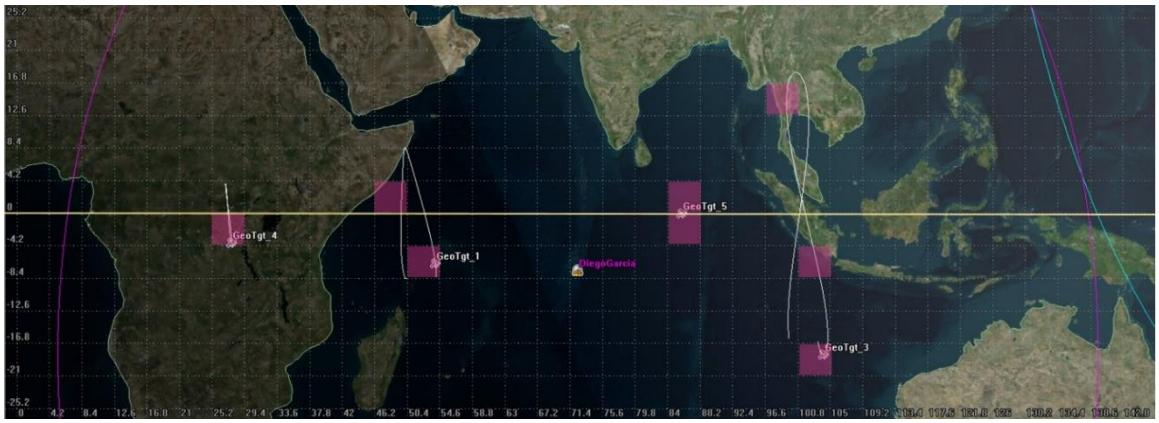

Figure 10: Concept of Coverage Area Calculation for Task-Based Scheduler

Latency

The evaluator uses the interval/access matrix generated in the scheduler to produce the performance values for minimum detectable size and latency. Values were produced by using the evaluation method similar to the Stern and Wachtel (2017) and Felten (2018) thesis. Their method produced a mean minimum RSO diameter for all observations and the latency. The method for determining the latency can be found in Stern and Wachtel (2017) thesis, pp 58–62. Stern and Wachtel calculated latency by using the mean of the maximum observation time gap. As an example in Figure 11, time gap "B" would be used as the maximum time gap for RSO #1, time gap "H" would be used for RSO #2 and then averaged with the rest of the 813 RSO's maximum time gaps.

In this thesis, latency is simply the average of all time gaps for all RSOs. From Figure 11, time gaps A-I are added to the rest of the 813 RSO's time

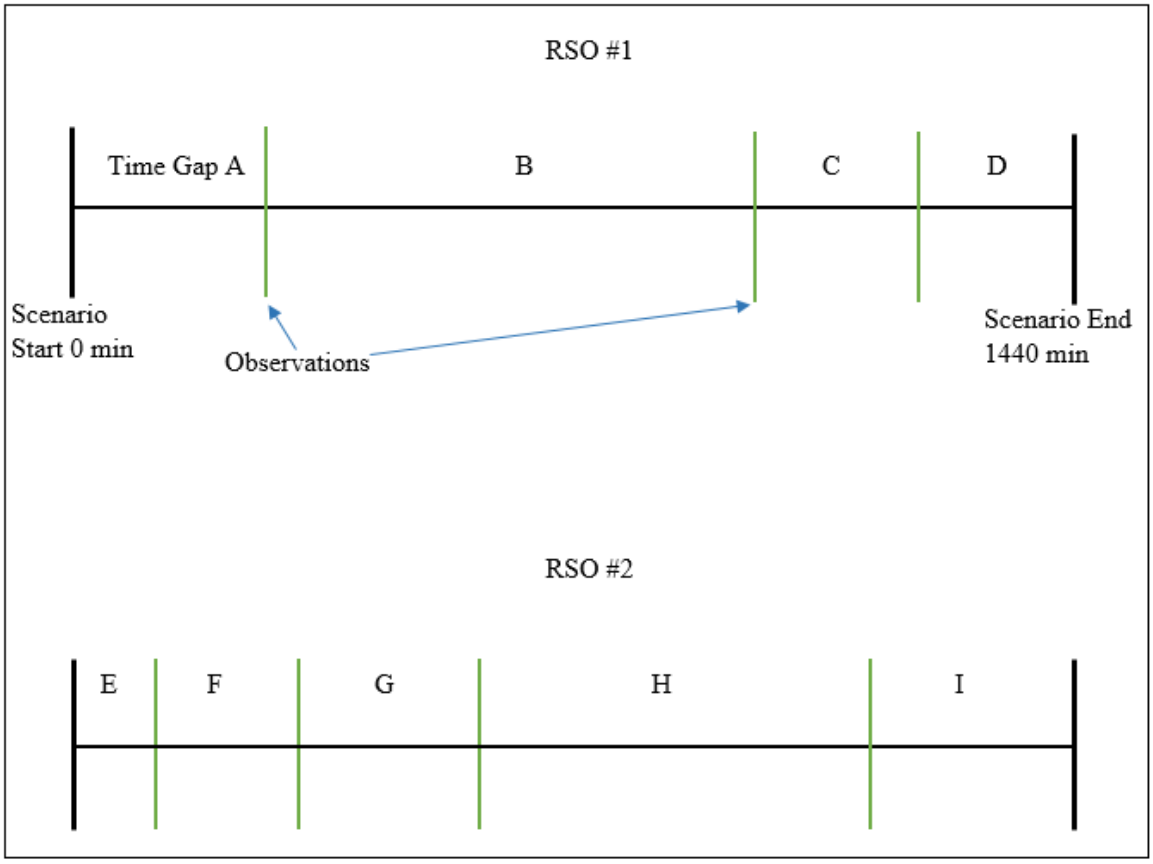

Figure 11: Example of Time Gaps for Latency Calculation

gaps and then averaged. RSOs that were unable to be viewed because of gaps in the simulated coverage were excluded from the calculation. Latency is calculated using Equation (8),

$$Latency\ (min) = \frac{\sum RSO\#1\ gaps + \sum RSO\#2\ gaps + \cdots \sum RSO\#n\ gaps}{Total\ Number\ of\ Time\ Gaps} \quad (8)$$

Assumptions

Two additional assumptions are made in the methodology. First, the percent cloud free line of site was 100%. Second, an object can be observed as long as it is in the FOV

of the sensor at a particular time for the search method. No FOV edge effects were incorporated.

Summary

This chapter reviewed the methodology used to develop the performance values needed to compare the task-based and search-based surveillance techniques. It covered how each technique was modeled and how performance was evaluated. It also provided justification on values used in the performance evaluation. The following chapter will discuss the results of the executed models.

IV. Analysis and Results

Chapter Overview

This chapter will show the performance results for minimum detectable size, detection rate, coverage area, and latency. Each subsection will discuss the performance metric and give explanations on observed performance trends and differences as independent variables were changed. It will also discuss how useful the performance metrics were in determining the best method.

Minimum Detectable Size

Minimum detectable size is the smallest size RSO the telescope would be able to detect, at the observed range, elevation angle, and solar phase angle, with a sensor capable of seeing objects as faint as 18 visual magnitude. Approximate size can be calculated for each observation by solving Equations (1–3) from Chapter III for the radius. The radius is then converted to a diameter. Table 1 shows the results for the average minimum detectable diameter for the various GEO belt inclination searches and time of year. As described in Chapter III, six inclination searches were evaluated up to +/- 16.97º.

The results show that on average the search method can see slightly smaller objects than the baseline tasking method. On each of the days every type of inclination search produces a better size than the tasking method. This confirms the hypothesis mentioned at the beginning of Chapter III. The reason searching can see smaller objects

could be that it better follows the anti-solar point[5], than the task-based approach. The tasking approach slews randomly around the GEO belt, and may not get many observations at optimal phase angles. With search, several observations will be taken at or near the anti-solar point with each scan of the night sky.

Table 1: Minimum Average Detectable Size Diameter in Centimeters

	21 June 2018	22 Sep 2018	21 Dec 2018	Average
Baseline Tasking[6]	45.2	47.9	49.6	47.6
Search[7] +/- 16.97º	34.1	36.2	44.6	38.3
Search[7] +/- 12.73º	41.3	40.2	39.4	40.3
Search[7] +/- 8.48º	40.6	39.9	46.7	42.4
Search[7] +/- 4.24º	41.2	43.1	45.3	43.2
Search[7] +/- 2.12º	42.3	46.0	45.9	44.7
Search[8] +/- 0.71º	42.4	46.7	47.0	45.4
Average	40.3	42.0	44.8	

Another trend discovered was minimum detectable size was the best at the summer solstice and got worse as it went towards the winter solstice even though atmospheric attenuation is higher in the summer. The average size across all methods for 21 Jun, 22 Sep and 21 Dec was 40.3 cm, 42.0 cm and 44.8 cm respectively. This trend is due to the locations of the simulated network of telescopes used. Two of the three telescopes are located at northern latitudes and the third is only a few degrees south of the equator. In the summer the network has better solar phase angles during the night due to

[5] Anti-solar point is the point on the celestial sphere directly opposite the Sun from an observer's perspective
[6] Single telescopes with 1.4ºx1.4º FOV (Latitude x Longitude)
[7] Three telescopes with combined 4.2ºx1.4º FOV (Latitude x Longitude)
[8] Three telescopes with combined 1.4ºx4.2º FOV (Latitude x Longitude)

the tilt of the Earth and the majority of observations coming from northern latitude telescope locations.

A third trend is that the minimum detectable size is somewhat insensitive to the search areas utilized. Generally minimum detectable size increases as the inclination search area decreases, however at the +/- 8.48º search on 21 Jun and 22 Sep, and the +/- 12.73º and +/- 4.24º searches on 21 Dec, the minimum detectable size decreased.

The last trend identified is minimum detectable size generally gets larger as the inclination search area gets smaller. This shows that the best method to get the smallest overall minimum detectable size is to use the +/- 16.97º search pattern. A reason for this could again be that the +/- 16.97º search area follows the anti-solar point better than the other inclination searches. As the search area decreases, the rate at which the search progresses across the sky gets faster causing it to take more observations away from the optimal anti-solar point. In addition, starting in the eastern part of the sky each night gave the smallest average detectable size. Appendix B shows the tables for the results when shifting the starting point of the searches westward. Starting searches in the East allows the search to start closer to the anti-solar point creating better phase angles resulting in smaller overall detectable size performance.

Detection Rate

Detection rate is the percent of RSOs that get at least one observation out of the total number of RSOs that are in the network FOV. Recall that 813 GEO RSOs are simulated, however only 722 RSOs on 21 Jun, 728 on 22 Sep, and 730 on 22 Dec are in the network FOV. Percentages are calculated on the number of viewable RSOs. Table 2

shows the results for detection rates with the different surveillance methods and time of year averaged over the ten different starting positions for each site. Appendix B shows the detection rates for each of the ten starting positions. As an example, the search method with a +/- 16.97º search area on 21 June observes had an average detection rate of 96.4% over the ten starting locations. This excludes the RSOs that are in the network's coverage gap. Unlike the minimum detectable size, the detection rate does not appear to get better or worse with a western or eastern starting point.

Table 2: Detection Rates

	21 June 2018	22 Sep 2018	21 Dec 2018	Average
Baseline Tasking	100%	100%	100%	100%
Search +/- 16.97º	96.4%	96.7%	97.4%	96.8%
Search +/- 12.73º	96.4%	95.8%	97.8%	96.7%
Search +/- 8.48º	95.5%	94.0%	97.2%	95.6%
Search +/- 4.24º	95.0%	92.9%	97.0%	95.0%
Search +/- 2.12º	92.8%	91.7%	96.5%	93.7%
Search +/- 0.71º	90.1%	89.2%	95.7%	91.7%

The baseline tasking method observes 100% of the RSOs in the FOV due to the nature of the 30-second greedy scheduler and the assumption of a cloudless night. The tasking scheduler observes the RSO that has the longest un-observed time, therefore all RSOs in the network FOV eventually get one observation. As hypothesized, the tasking method performs better than the search method in regards to detection rate.

A noticeable trend is detection rate decreases as the inclination search area gets smaller. As seen in the rightmost column of Table 2, the average detection rate across the three dates is steady at the +/- 16.97º and +/- 12.73º searches but then begins to decline as

the searches area gets smaller. Intuitively this make sense; as inclination search area decreases, the chance of seeing higher inclined RSOs decreases. Figure 12 shows the inclination distribution of the 813 RSOs used in the model. The bulk of the RSOs are below 16º. Although more passes are made across the sky as the search area decreases, which makes more opportunities for detections, it is not enough keep the detection rate from dropping.

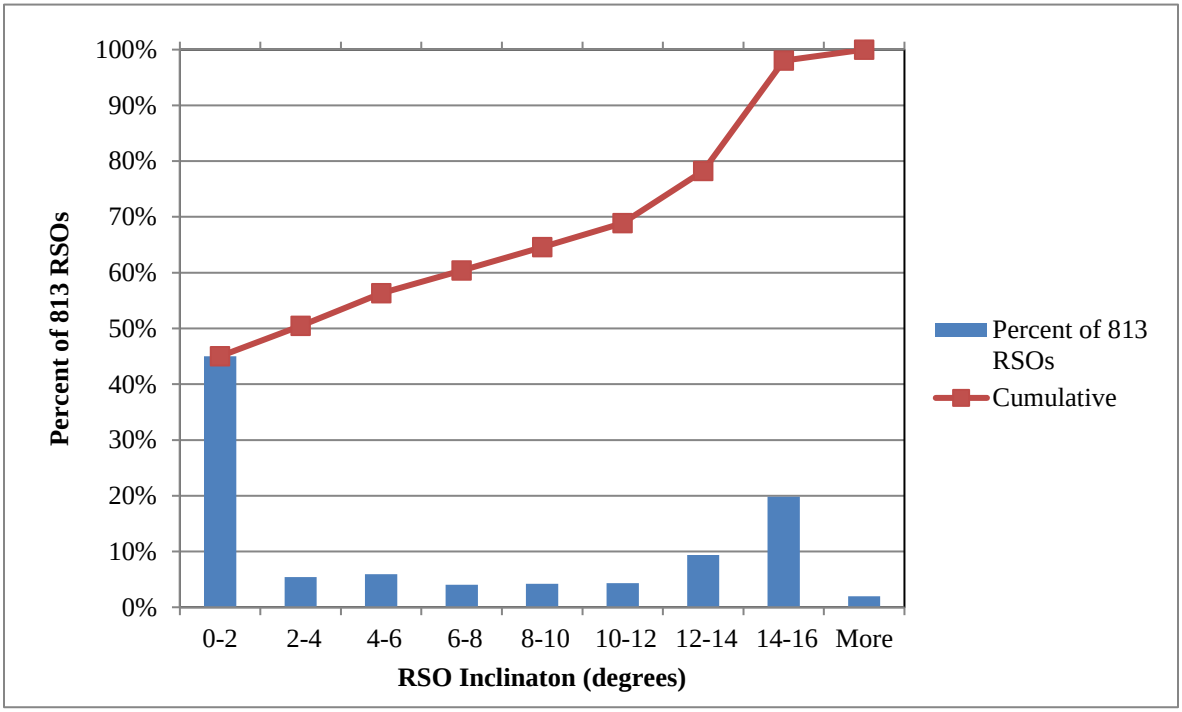

Figure 12: Inclination Distribution of the 813 RSOs

Coverage Area

Coverage area is the amount of area between +/- 16.97º above and below the equator that gets observed by the telescope as explained in Chapter III. Figure 13 shows the graph of the coverage area percent vs. the number of RSOs used in the scenario.

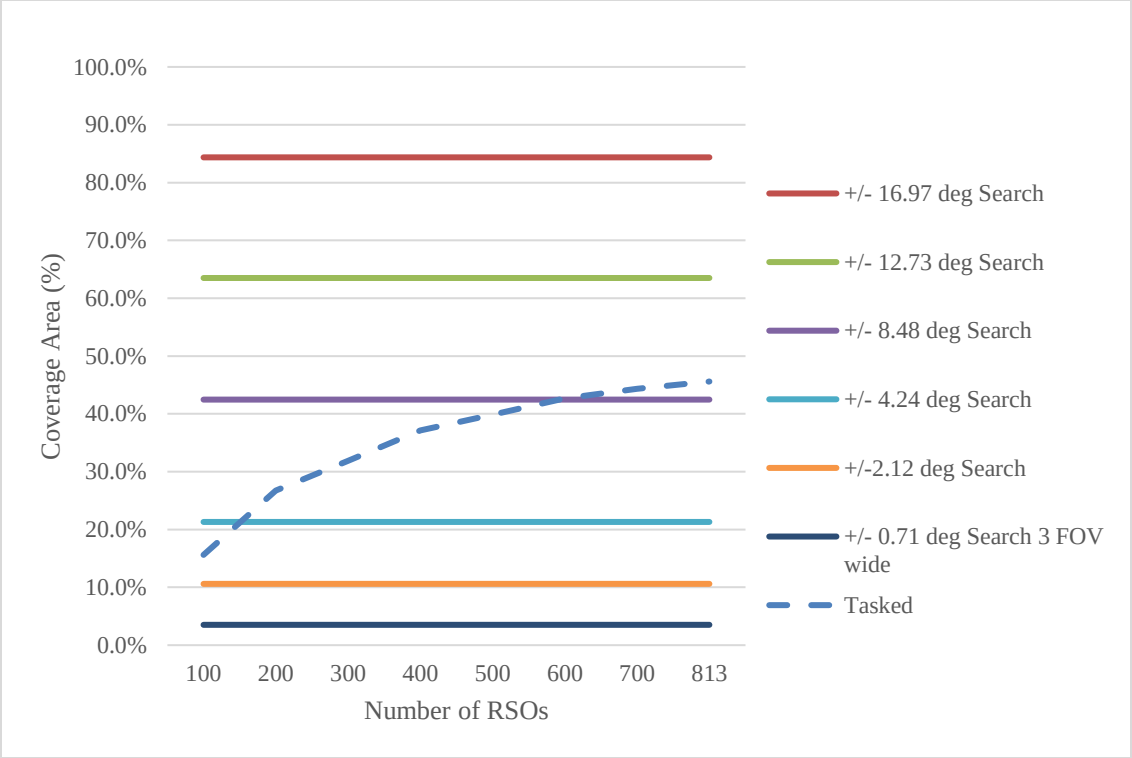

Figure 13: Comparison of Tasked-Based Coverage vs. Different Search Methods

The graph shows that search coverage area does not change as the number of RSOs in the model are added. The search will cover the same amount of sky no matter how many RSOs are in the scenario. The search method has a max coverage of 84.4% at the +/- 16.97º search since the network has a coverage gap over the Atlantic Ocean. The gap can be seen on the right and left edges of Figure 9. Coverage area obviously goes down as the inclination search area is narrowed. Tasking coverage area increases as more RSOs are added to the model, but it levels off at about 46%. The more RSOs that are available to observe, the more of the sky is viewed which is reflected in the graph. However, this trend tapers off as seen by the flattening of the task-based curve. This flattening is due to the inclinations of the 813 RSOs used. Recalling Figure 12, the majority of RSOs have inclinations less than 6º. Most task-based observations will be made within 6º of the

equatorial line. The task-based method has very few opportunities to view RSOs at higher inclined areas. Also, the coverage area did not change with respect to the time of year for either search or task mode. The search method has better coverage than the task method with the +/- 16.97º and +/- 12.73º searches but not at the smaller search areas.

However, when looking at the detection rate results in the previous section and considering that every RSO in GEO crosses the equatorial line, it is apparent that coverage area is not a good discriminator for performance unless searching "blank space" is important for SSA[9]. Even though coverage area is only 3.5% for the +/- 0.707º three wide search, the search strategy still acquires observations on about 92% of the possible RSOs in the network FOV. This shows that having the largest coverage area (84.4%) marginally improves detection rate (98.6%). A major drop in coverage area (3.5%) does not correlate to a major drop in detection rate (91.7%). The next section shows that a smaller search area does improve the latency.

Latency

Latency is simply the time between observations of a particular RSO. Table 3 shows the results for latency with the different surveillance methods and time of year averaged over the ten different starting positions for each site. Appendix B shows the detection rates for each of the ten starting positions for the search method. Like the detection rate, latency does not appear to get better or worse with a western or eastern starting point. Several trends can be seen from the results.

[9] Finding new smaller objects will require searching "blank space"

Table 3: Latency Results for Task and Search Methods in Minutes

	21 June 2018	22 Sep 2018	21 Dec 2018	Average
Baseline Tasking	84	78	72	78
Search +/- 16.97º	488	487	433	469
Search +/- 12.73º	428	428	371	409
Search +/- 8.48º	354	357	304	338
Search +/- 4.24º	239	237	204	227
Search +/- 2.12º	152	150	129	144
Search +/- 0.71º	65	65	55	62

The first trend is generally that as the nights get longer from June to Dec, the latency goes down. As mentioned earlier, due to the northern latitude location of two of the three telescope sites, longer observation times for the network happen in the winter. The longer nights allow for more observations to be made bringing down the overall latency.

The second trend is the overall latency improvements are greater from 22 Sep to 21 Dec than from 21 Jun to 22 Sep. The latency for the +/- 8.48º search actually increases from 21 June to 22 Sep. This increase in latency and difference in improvements is from the 22 Sep date being in the middle of eclipse season. Eclipse season is when the Earth passes between the RSO and the Sun from 26 Feb to 13 Apr and from 21 Aug to 15 Oct. This causes RSOs to be un-viewable with optics during periods of the night.

The third and most obvious trend is latency improves as the search area is decreased. As the search area gets smaller the telescopes can make more passes across the sky. More observations are made as the number of passes increases, thus lowering the

overall latency. In this scenario with 813 RSOs, the search method outperforms the tasking method but only with the +/- 0.71º three FOVs wide search area.

The last two trends are shown in the latency results depicted in Figure 14. The graph is the average latency over the three days vs. the number of RSOs in the scenario. The graph shows that search latency stays fairly constant for each inclination search area as the number of RSOs in the scenario increases, while the tasking latency increases linearly as number of RSOs are increased. A linear fit to the tasking results gives the following Equation (9) for latency.

$$Tasked\ Latency\ (\text{min}) = 0.096544x\ +\ 0.8712 \tag{9}$$

where,

x is the number of RSOs in the scenario

Keep in mind the graph is the average latency of the eastern most starting positon and not an average over all ten starting positions.

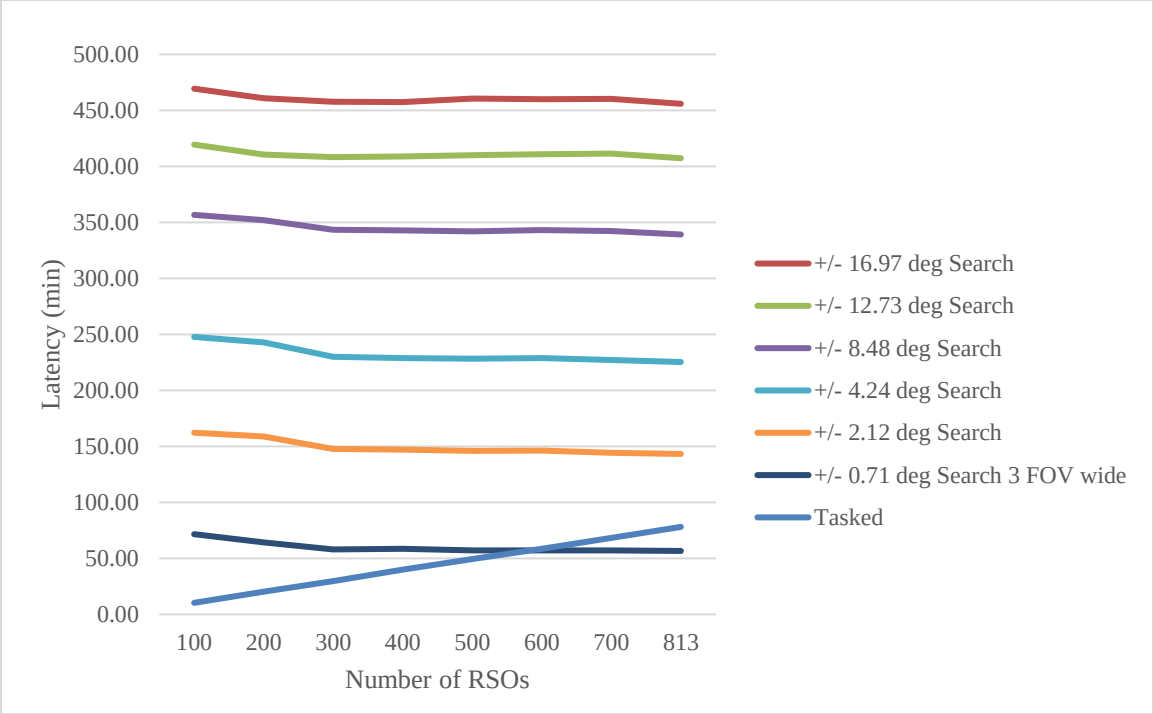

Figure 14: Average Latency vs. Number of RSOs in a Scenario at the Eastern Starting Position

For each of the other search areas greater than the +/- 0.71º three FOVs wide method, the latency is greater than the tasking method. However, for each of these search areas there is an approximate crossover point at which the tasking method will have longer latency than the search method. As an example the +/- 4.24º inclination search area will be used to estimate the crossover point. Using the Equation (9) and a latency of 227 minutes, average latency for the +/- 4.24º search across the three dates, solve for the approximate number of RSOs that would be the crossover point for latency performance. The crossover point is 2,343 RSOs with the assumption they have the same distribution in GEO as the 813 RSOs used. This means the task-based method performs better than the +/- 4.24º search method up to 2,343 RSOs in the scenario. Anything over this

number, the search method has better latency performance. Table 4 presents the crossover number for each search method. Recall from Chapter II, NASA estimates there are more than 3,250 RSOs greater than 10 cm in diameter in GEO as of 2010 (Johnson, 2010). Using NASA's estimate for GEO population the crossover point for latency performance would be close to the +/- 8.48º search area. Again, this is assuming the same distribution of orbital elements for the additional RSOs as the 813 RSOs used in this model. Actual RSO orbital element distributions would likely be different and produce different results.

Table 4: Latency Crossover Points Where Search-Based Method Will Outperform Task-Based

Search Area	+/-16.97º	+/-12.73º	+/-8.48º	+/-4.24º	+/-2.12º	+/-0.707º 3 wide
Number of RSOs	4,860	4,235	3,506	2,349	1,489	641

Latency is calculated by taking the average of all the time gaps. When taking an average it is important to look at the distribution of the data. There was some concern that time gaps representing daytime gaps would dominate the distribution. Appendix C shows the distributions of time gaps for the task method and searching methods. For the task method 93% of the time gaps were less than two hours while the time gaps that represented daytime, ten hours and greater, were at most 4% of the total time gaps. For the +/- 16.97º search method, daytime gaps represent 20–25% of the total time gaps. There is a visible increase in frequency at the 10–14 hour bins for the +/- 16.97º search method on the histogram graph. This representation decreases as the search areas get

smaller and number of shorter time gaps increase due to the increased number of observations.

Relevant Research Comparison

Recalling Chapter II, Choi found that their method for surveying had detection rates of 90% and 95% for non-operational and operational RSOs respectively. Choi used 287 RSOs over a single site located in South Korea and used an up and down scanning pattern within a +/-17º search area. (Choi et al., 2015). Flohrer's model used 4 locations placed around the world with 793 simulated RSOs. Flohere simulated "strip" scanning, constraining the search area to +/-17º, and obtained detection rates of 89.8% and 94.7% for 8-hour and 12-hour observations per night respectively similar to Choi's detection rates. Flohrer's research also determined objects could be seen down to 25 cm in diameter (Flohrer et al., 2005).

This thesis used a similar search pattern and search area as Choi, and found similar detection rates ranging from 91.7% to 96.8%. This research expanded the scope by using 813 RSOs with a network of three locations and multiple telescopes at each location. This thesis found minimum detectable size averages of 38–48 cm in diameter. This research went beyond the previous researcher's results by adding ways to measure a search-based space surveillance method by calculating latency and coverage area.

Summary

This chapter described the performance results for minimum detectable size, detection rate, coverage area, and latency. The results showed that the search method performed slightly better in minimum detectable size. Tasking had better detection rates.

Search had better coverage area with the larger search areas but because of the dynamics of GEO RSOs and detection rate results, coverage area is deemed not to be a good discriminator. The +/- 0.71º three FOVs wide search method had shorter latency than tasking for this model with 813 RSOs. It was also found that each search method has a crossover point with respect to number of RSOs in the scenario at which latency is roughly equal.

V. Conclusions and Recommendations

Chapter Overview

This chapter begins with answering the research questions stated in Chapter I and the significance of findings. Next, recommended actions on how to use the results to perform operations better will be discussed. Finally, areas for future research and model improvement will be presented.

Research Questions Answered

1. *How does switching from tasked based to search-based space surveillance affect GEO SSA performance?*

Search was consistently better than tasking when it came to minimum detectable size. The +/- 16.97º search was able to detect objects 5-11 cm smaller than the task method, depending on the time of year. The smaller searches all performed better than task-based too but by smaller margins.

The tasking method had better detection rates, as hypothesized, than any search method. Due to the nature of the tasking scheduler and assumption of cloudless skies, the tasking method had a 100% detection rate. The best search method produced an average detection rate of 96.8% over the three dates with a max detection rate in the winter of 97.8%.

The search method had a better coverage area with a maximum coverage of 84% while the tasking method had roughly 46%. However as discussed in Chapter IV coverage area is not a good discriminator of performance.

The +/- 0.71º three FOVs wide search had the shortest average latency performance with an average of 62 minutes. The tasking method had an average of 78 minutes. The +/- 0.71º three FOVs wide search area was the only search method that had better latency performance than the tasking method.

2. *How do different search patterns and constraints affect performance?*

For minimum average detectable size the best performance came from the +/- 16.97º inclination search area. In general as the inclination search area decreased, the minimum detectable size increased. Figure 15 shows the graph of how size changes with search area thickness. There were some exceptions to this when looking at certain dates and search areas but averaging across the dates, the minimum detectable size increased as inclination search area decreased as reflected in Figure 15. It was also found that starting each search in the eastern sky produces the smallest detectable sizes. Size did not change with respect to the number of RSOs in the model.

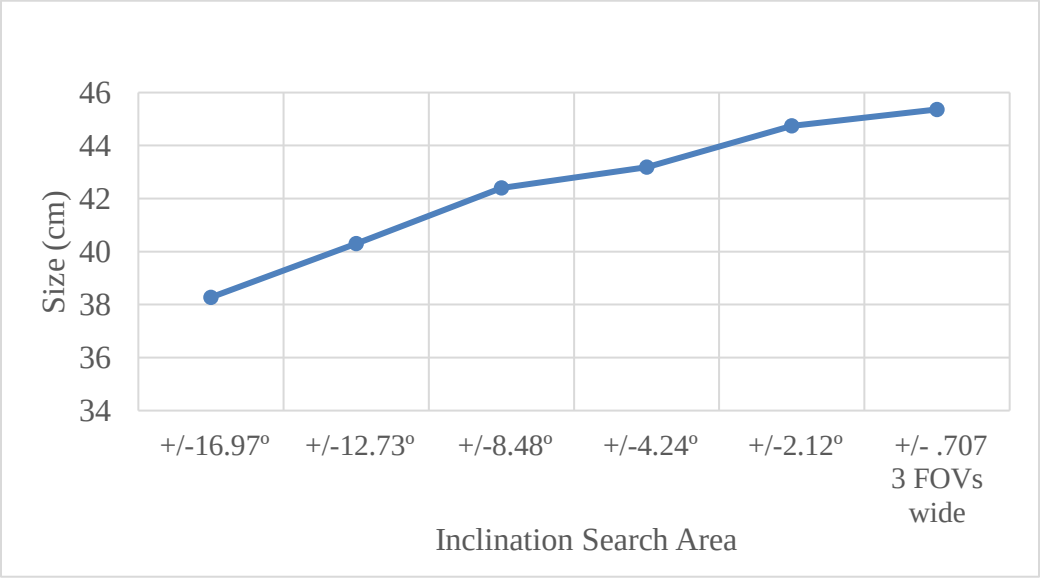

Figure 15: Minimum Average Detectable Size vs. Inclination Search Area

The +/- 16.97º and +/- 12.73º searches were roughly identical with the two highest detection rates among search areas. However, shrinking the search areas any further causes the detection rate to also decrease. Figure 16 shows how detection rate is sacrificed after the search area gets smaller than +/- 12.73º. Detection rate did not have any relationship to where the search started in the sky nor did it vary with respect to how many RSOs were in the model.

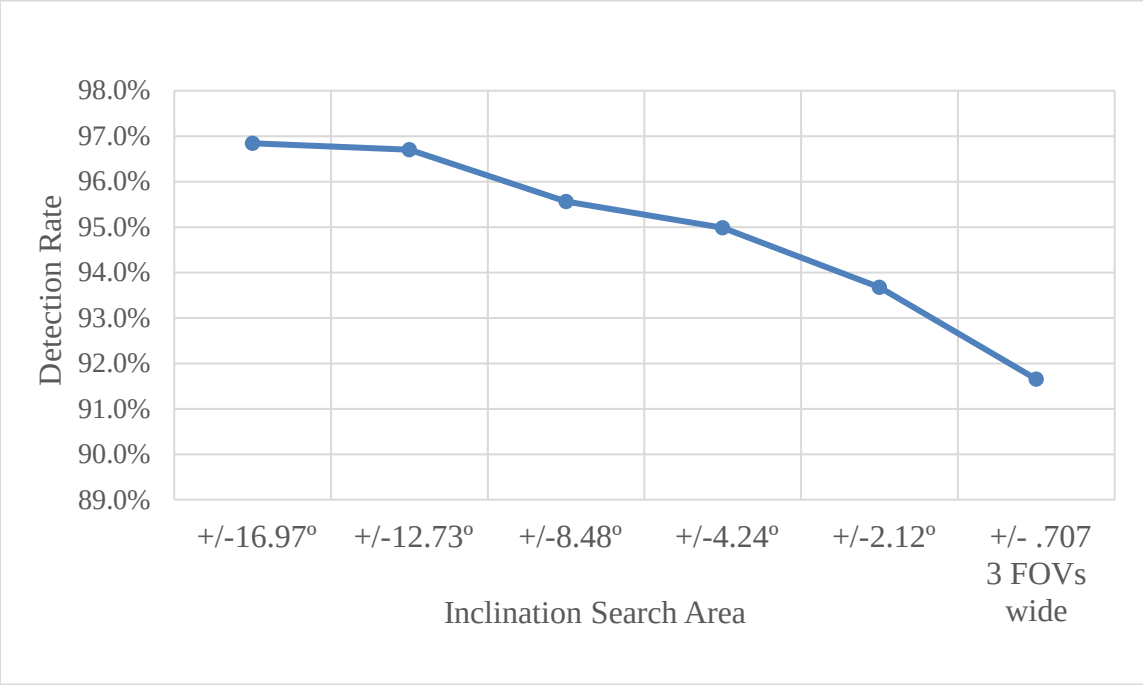

Figure 16: Detection Rate vs. Inclination Search Area

From Figure 13 in Chapter IV, coverage area decreases as the search area decreases. Coverage area did not change as search starting positions changed nor did they change as the number of RSOs in the model changed. Coverage area is simply a function of the search area thickness but as stated earlier, coverage area is not a good performance metric for comparison.

As inclination search area decreases, latency decreases. Figure 17 shows how the average latency changes with thinner search patterns. Latency did not have any relationship to where the search started in the sky nor did it vary with respect to how many RSOs were in the model as seen previously in Figure 14. Latency holds steady as the number of RSOs in the model increases past 300.

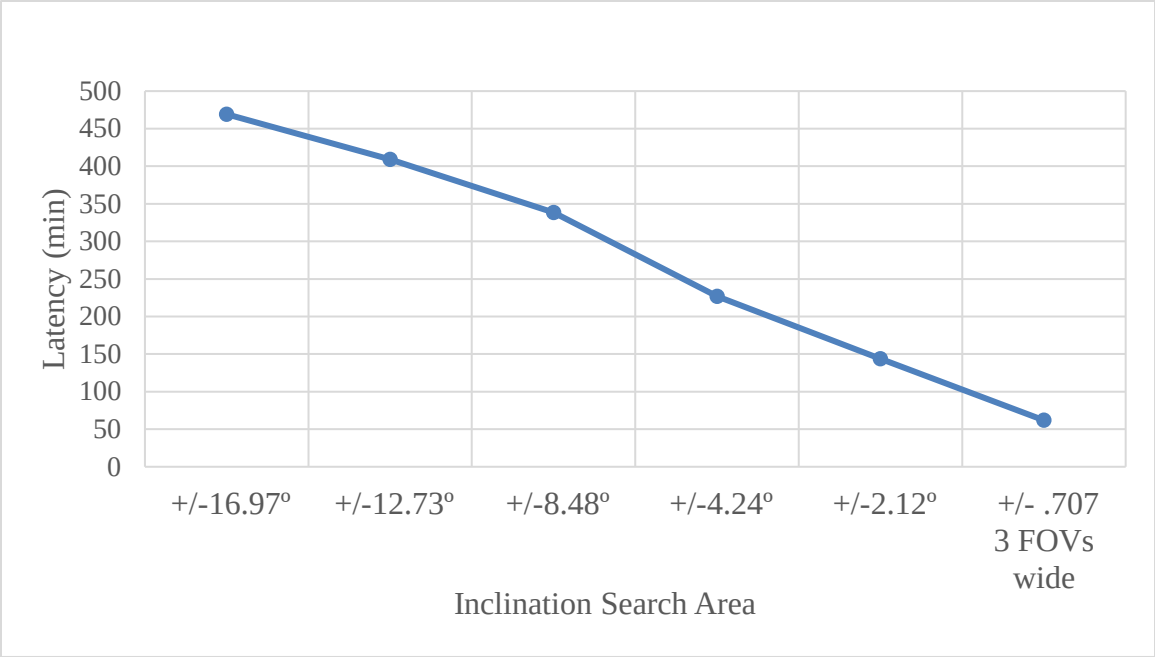

Figure 17: Latency vs. Inclination Search Area

Significance of Research

The significance of this research is that new ways of ground-based telescope space surveillance operations can be modeled and assessed for performance. This research can provide answers on how to best utilize current US space surveillance ground-based telescopes. It can help provide insight into the advantages and disadvantages to new ways of performing space surveillance with ground-based telescopes without having to perform costly tests and take away from operational time.

This research could also be applied to other networks of ground-based telescopes that want to find ways to improve their surveillance performance.

Recommendations for Action

A best value decision matrix was used to choose the best method based on minimum detectable size, detection rate and latency. The decision matrix gave equal weights to each of the three performance metrics. Coverage area was not used in the decision matrix since it was not a good discriminator of performance. Value scores from 0 to 1 were given to each performance metric for the task-based and search-based methods. Minimum detectable size was given values on a linear scale from 10 cm to 100 cm with a value score of 1 for 10 cm or smaller and 0 for 100 cm and larger. Detection rate was given values on a liner scale from 75% to 100% with a value score of 1 for 100% and 0 for 75% and lower. Latency was given values on a linear scale from 30 minutes to 600 minutes with a value score of 1 for 30 minutes or less and a 0 for 600 minutes or more. Appendix E contains the graphs and linear equations that depict how the values were assigned based on performance. Table 5 shows that the task-based method has the highest overall value when performance is equally weighted.

Table 5: Decision Matrix Values

	Size (cm)	Size Value	Detection Rate	Detection Value	Latency (min)	Latency Value	Value
Baseline Tasking	47.6	0.583	100.0%	1.000	78	0.912	0.832
Search +/- 16.97º	38.3	0.686	96.8%	0.872	469	0.208	0.589
Search +/- 12.73º	40.3	0.664	96.7%	0.868	409	0.316	0.616
Search +/- 8.48º	42.4	0.640	95.6%	0.824	338	0.444	0.636
Search +/- 4.24º	43.2	0.632	95.0%	0.800	227	0.644	0.692
Search +/- 2.12º	44.7	0.615	93.7%	0.748	144	0.793	0.719
Search +/- 0.71º	45.4	0.607	91.7%	0.668	62	0.941	0.739

However, at some point there will be too many objects for the tasking method to outperform a search-based method in latency and detection rate. As seen from Chapter I the number of objects in GEO has been increasing at a rate of two additions to one removal each year from 2000 to 2009 and there are over 3,250 objects in GEO greater than 10cm as of 2010 (Johnson, 2010). In the future, if the GEO catalog expands to a few thousand objects then either more telescopes would have to be built or a searching or scanning technique would be needed. If the catalog expanded to approximately 10,000 RSOs or more in GEO, depending on the time of year and distribution of added RSOs, the tasked-based method would not have enough time to make an observation on every RSO in a single night which would cause a decline in detection rate.

On the other hand, switching to a 100% search method may not be the full answer to providing the best ground-based space surveillance. The ultimate goal of SSA is to know where everything is at all times. No search method was able to detect 100% of the possible objects each night. Choosing the largest inclination search area does produce a detection rate close to 97% and has the best minimum size detection but it also has the worst latency performance of any method. Shrinking the inclination search area would decrease latency but would also decrease the detection rate.

It is very possible that a combination of task-based and search-based surveillance could be used to get the best performance. The smallest inclination search area could be used for the first portion of the night with a follow up of taskings that could get observations on RSOs that were missed during the search. This is an area of future work discussed in the next section. The combination of search-based and task-based surveillance is also recommended by studies discussed in Chapter II.

Recommendations for Future Research

This section lists and discusses recommendations for follow-on work and future research. There are many ways the modelling and simulation can be improved to gain a more accurate picture of the true advantages and disadvantages of task-based and search-based space surveillance. Below is the list of recommendations and their explanations in order of importance.

1. Add weather effects.
2. Improve the schedulers by integrating slewing rates and more accurate imaging time.
3. Analyze different search patterns and how to mix search and task.
4. Add RSOs outside of the GEO region and different distributions of RSOs.
5. Simulate additional telescope locations and numbers of telescopes.
6. Examine changes in telescope FOV.
7. Simulate unknown RSOs and more RSOs.

These are described below:

1. Weather. This thesis assumes cloudless skies and perfect weather conditions for viewing each night. In reality ground telescopes cannot operate during high winds or rain and they are unable to see through clouds. Adding weather and simulated cloud cover for each of the site locations would add fidelity to the model. With weather, multiple simulations can be run and statistical analysis can be done on the results.

2. Scheduler Improvements. The task-based scheduler used in this thesis is a simple greedy algorithm that takes an observation on the RSO that has not been

observed in the longest time. Adding in a prioritization list to emulate the real-world task list would help make the model more realistic. The current task-based model does account for good viewing angles. Putting in priority for observing RSOs with good viewing angles would also help emulate real-world operations. The model for both schedulers uses 30 seconds to complete observations which is conservative. Incorporating slewing rates and actual imaging times will add fidelity to the model. Finally, the task-based scheduler does not give credit for observing other RSOs that happened to be in the same FOV as the RSO being observed. Although this is how current real-world operations are performed, adding the ability to credit observations for other targets in the FOV could help with future research on how current operations could be cost effectively improved.

3. Search patterns and mixing Search and Tasking. In this thesis the search-based scan pattern followed a downward motion and then moved over a FOV to start at the top of the search area with another downward sweep. Using different search patterns could produce different results. For example, simulating a search pattern that follows the anti-solar point could help improve performance in minimum detectable size. Other patterns like a snaking pattern, strip scanning across longitudinally, or small box area searches would produce different results. One option could be to mix search-based and task-based methods. This thesis and several studies mentioned in Chapter II recommend that some sort of search-based and task-based methods are needed for better SSA.

4. Different RSOs. The model is limited by only using 813 GEO RSOs. There are an estimated 3,250 objects greater than 10 cm in GEO. However, deep space ground-based telescopes are tasked with getting observations on RSOs in other regions. Adding in simulated Highly Elliptical Orbit (HEO) or even some Medium Earth Orbit (MEO) RSOs can add some fidelity to the model. Also trying different distributions of RSOs in GEO would have an effect on performance.

5. Telescope locations and numbers. This thesis used a network of telescopes and the currently reported locations, modeled after the existing GEODSS architecture. The same methods and analysis could provide performance estimations of new potential sites to build. Also varying the number of telescopes at each site could be done. Referencing the Stern and Wachtel (2017) and the Felten (2018) optimization models would be good for varying site locations (up to 9) and varying the number of telescopes at each site (up to 4).

6. Telescope Field of View (FOV). The FOV used for each telescope in this research was modeled after the existing deployed hardware. Future work could look at varying the size of the FOV to see how much performance changes. This would be good for decision makers wanting to predict the value of upgrading optics.

7. Simulate unknown RSOs and more RSOs. One of the motivations for switching to a 100% search-based surveillance method was the concern that the task-based approach is not able to see objects that are not on the task list. In this thesis all objects are known to the task-based method which is the reason it has 100% detection rate. Modeling unknown RSOs in the task-based method would

shed light on the true task-based detection rate. Also adding in more RSOs would increase the fidelity of the model by emulating the actual number of RSOs in GEO, and it could help confirm the crossover points found in Chapter IV.

Summary

This chapter answered the research questions presented in Chapter I, discussed the significance of the research, recommended operational actions, and presented areas for future research and improvements to the model used in this thesis. At the present number of about 850 RSO being tracked it appears that a task-based approach is the best method for ground-based space surveillance. However, the actual number of RSOs in GEO is estimated to be four times that amount and it continues to grow. To increase SSA capacity and get closer to persistent SSA, switching to a search-based method has shown to be beneficial.

Appendix A

This Python code converts the local reference frame observation data (azimuth, elevation, lat/long, semi major axis) to a global latitude/longitude location of RSOs for each of the ground station locations.

```
"""
Created on Mon Aug 13 10:57:02 2018

@author: fhertwig
"""
import math
def azi_dist_to_coord(lat1,lon1,el,azi,semimajor):
    #change degree values into radians
    lat1=math.radians(lat1)
    lon1=math.radians(lon1)
    el=el+90 #add 90 deg to elevation to get the earth center,facility,target angle
    el=math.radians(el)
    azi=math.radians(azi)

    centerangle=math.pi-(math.asin((math.sin(el)/semimajor)*6371)+el) #angle of facility,earth center,target

    #calculates the second lattitude
    lat2=math.asin((math.sin(lat1))*(math.cos(centerangle))+(math.cos(lat1))*(math.sin(centerangle))*(math.cos(azi)))

    #calculates the second longitude
    lon2=lon1+math.atan2(math.sin(azi)*math.sin(centerangle)*math.cos(lat1),math.cos(centerangle)-math.sin(lat1)*math.sin(lat2))

    #convert back to degrees
    lat2=math.degrees(lat2)
    lon2=math.degrees(lon2)

    return (lat2,lon2)

print azi_dist_to_coord(33.8200,-106.66,15,132.03,41964)
```

Appendix B

The tables below show the results for each search area when the search is started at different locations in the sky. Search starting positions were equally spaced across each site's FOV. The first starting position starts in the eastern sky (.0) for each site location and then shifted west over to the next starting position (.1–.9). The 10 different starting positions provide more data points to make sure consistent values were being found for size, latency and detection rate.

Minimum detectable size (cm)						
21-Jun						
	16.97º	12.73º	8.48º	4.24º	2.12º	3 wide
Size with shift of .0	34.06	41.32	40.57	41.16	42.32	42.4
Size with shift of .1	36.63	40.66	40.95	41.54	42.25	42.5
Size with shift of .2	39.91	40.22	43.07	42.59	42.26	42.72
Size with shift of .3	44.48	40.13	44.21	43.99	43.10	42.80
Size with shift of .4	47.71	40.90	44.76	44.94	43.85	42.81
Size with shift of .5	47.71	45.00	44.92	45.42	44.05	42.77
Size with shift of .6	47.35	46.65	46.39	45.32	44.09	42.70
Size with shift of .7	47.01	48.86	47.31	45.11	44.11	42.64
Size with shift of .8	46.27	51.04	47.19	44.58	43.93	42.73
Size with shift of .9	44.30	48.92	45.15	43.31	43.42	42.69

Minimum detectable size (cm)						
22-Sep						
	16.97º	12.73º	8.48º	4.24º	2.12º	3 wide
Size with shift of .0	36.2	40.2	39.94	43.09	45.97	46.72
Size with shift of .1	42.32	39.71	39.66	43.13	46.34	46.75
Size with shift of .2	47.14	39.51	44.01	43.32	46.42	46.73
Size with shift of .3	48.45	40.58	47.65	45.25	46.57	46.73
Size with shift of .4	50.12	42.65	48.16	45.62	46.79	46.70
Size with shift of .5	51.60	50.73	47.61	47.15	46.70	46.63
Size with shift of .6	51.87	52.83	47.36	48.14	46.51	46.52
Size with shift of .7	49.70	51.99	47.73	48.29	47.43	46.44
Size with shift of .8	47.66	51.37	47.60	47.76	47.82	46.72
Size with shift of .9	44.08	49.85	46.04	46.31	47.79	47.11

Minimum detectable size (cm)						
21-Dec						
	16.97º	12.73º	8.48º	4.24º	2.12º	3 wide
Size with shift of .0	44.56	39.39	46.67	45.31	45.94	46.97
Size with shift of .1	43.83	41.92	46.29	46.19	46.31	47.09
Size with shift of .2	44.55	46.56	45.56	46.79	46.60	47.08
Size with shift of .3	46.63	47.82	45.41	47.12	47.14	46.99
Size with shift of .4	47.44	48.32	45.62	47.64	47.89	47.00
Size with shift of .5	48.64	48.25	45.59	48.66	48.06	47.05
Size with shift of .6	47.71	49.65	47.96	48.39	48.05	46.96
Size with shift of .7	44.82	51.84	48.97	48.02	47.73	46.94
Size with shift of .8	46.62	50.63	52.11	48.38	47.34	47.16
Size with shift of .9	49.22	46.60	50.60	47.47	46.64	47.07

Detection Rate						
21-Jun						
	16.97º	12.73º	8.48º	4.24º	2.12º	3 wide
Shift of .0	95.3%	94.3%	95.7%	95.2%	92.4%	89.6%
Shift of .1	95.8%	96.4%	95.8%	95.2%	92.8%	89.9%
Shift of .2	94.5%	96.5%	94.9%	96.0%	93.2%	90.4%
Shift of .3	96.5%	95.7%	95.6%	95.0%	94.0%	90.4%
Shift of .4	97.5%	96.5%	95.7%	93.8%	93.1%	90.0%
Shift of .5	97.2%	96.5%	95.4%	93.9%	92.2%	90.0%
Shift of .6	97.1%	97.5%	95.4%	93.9%	92.5%	90.0%
Shift of .7	97.4%	97.1%	95.3%	95.3%	92.8%	90.6%
Shift of .8	96.4%	97.5%	96.0%	95.8%	92.9%	90.0%
Shift of .9	96.7%	96.3%	95.6%	95.8%	92.2%	89.9%

Detection Rate						
22-Sep						
	16.97º	12.73º	8.48º	4.24º	2.12º	3 wide
Shift of .0	97.9%	93.0%	92.4%	95.3%	91.8%	89.3%
Shift of .1	98.5%	93.4%	93.8%	93.8%	92.3%	89.3%
Shift of .2	98.5%	94.8%	92.4%	92.7%	92.0%	89.1%
Shift of .3	97.8%	96.0%	92.9%	92.0%	91.8%	89.1%
Shift of .4	96.8%	96.2%	94.4%	91.8%	91.5%	89.0%
Shift of .5	94.0%	96.8%	95.5%	92.2%	91.1%	89.0%
Shift of .6	92.9%	97.4%	94.5%	91.6%	91.8%	89.0%
Shift of .7	95.1%	97.3%	95.5%	92.4%	91.9%	89.1%
Shift of .8	97.7%	97.0%	94.5%	92.7%	91.9%	89.4%
Shift of .9	98.1%	96.6%	93.7%	94.5%	91.3%	89.4%

Detection Rate						
	21-Dec					
	16.97º	12.73º	8.48º	4.24º	2.12º	3 wide
Shift of .0	97.4%	97.3%	97.0%	97.0%	96.6%	95.8%
Shift of .1	97.1%	97.5%	97.7%	97.4%	96.4%	95.8%
Shift of .2	97.4%	97.5%	97.3%	97.4%	96.3%	95.8%
Shift of .3	97.7%	97.5%	97.3%	97.5%	97.0%	95.5%
Shift of .4	97.8%	97.9%	97.8%	97.5%	96.6%	95.2%
Shift of .5	97.7%	97.8%	97.3%	96.7%	95.6%	95.3%
Shift of .6	97.3%	98.1%	96.7%	96.6%	96.2%	95.5%
Shift of .7	96.0%	98.5%	96.6%	96.7%	96.3%	96.0%
Shift of .8	97.7%	98.1%	97.0%	96.8%	96.8%	96.2%
Shift of .9	97.7%	97.9%	97.4%	96.7%	96.8%	95.8%

Latency (min)						
21-Jun						
	16.97º	12.73º	8.48º	4.24º	2.12º	3 wide
Shift of .0	484.3	431.8	355.2	238.4	151.6	64.9
Shift of .1	496.0	433.2	352.5	239.1	151.6	65.0
Shift of .2	510.6	432.3	354.4	240.7	152.2	65.0
Shift of .3	521.1	431.0	357.6	241.8	152.8	65.0
Shift of .4	496.3	424.7	353.3	241.1	152.8	65.1
Shift of .5	487.4	424.5	353.4	241.1	152.4	65.0
Shift of .6	478.9	421.6	354.6	240.8	152.1	65.0
Shift of .7	470.7	428.4	352.1	238.0	152.0	65.0
Shift of .8	466.2	423.5	352.4	236.5	151.4	65.0
Shift of .9	467.3	425.6	355.4	237.3	151.6	64.9

Latency (min)						
22-Sep						
	16.97º	12.73º	8.48º	4.24º	2.12º	3 wide
Shift of .0	466.8	426.3	360.2	235.5	149.6	65.2
Shift of .1	450.3	431.3	357.4	235.7	150.3	65.1
Shift of .2	437.3	439.0	354.8	236.7	150.4	65.3
Shift of .3	458.2	445.9	355.2	237.0	150.6	65.3
Shift of .4	503.8	445.3	357.8	238.4	151.0	65.4
Shift of .5	526.0	435.2	352.7	238.0	150.8	65.4
Shift of .6	547.7	418.2	351.7	238.9	150.0	65.4
Shift of .7	526.0	407.0	354.5	237.7	149.1	65.3
Shift of .8	480.7	407.6	358.5	237.8	149.0	65.3
Shift of .9	471.2	424.6	364.9	237.6	148.8	65.3

Latency (min)						
21-Dec						
	16.97º	12.73º	8.48º	4.24º	2.12º	3 wide
Shift of .0	420.3	365.9	302.1	202.7	128.8	55.2
Shift of .1	422.5	366.9	305.4	203.5	128.7	55.2
Shift of .2	425.8	362.7	304.1	203.2	129.2	55.3
Shift of .3	429.4	366.4	303.6	202.9	129.4	55.3
Shift of .4	440.4	371.6	303.8	203.9	129.8	55.3
Shift of .5	447.1	374.6	304.2	203.8	130.0	55.3
Shift of .6	445.2	378.1	306.1	204.3	129.5	55.3
Shift of .7	436.9	377.9	307.1	203.8	129.1	55.2
Shift of .8	433.5	373.8	304.5	204.0	128.4	55.2
Shift of .9	427.7	372.1	304.0	204.1	128.5	55.1

Appendix C

The graphs below show the distribution of time gaps for the task method and searching methods. The graphs show that task-based daytime time gaps are not a significant portion of the average latency. The search-based daytime time gaps are more prevalent in the larger search area but diminish as the search area decreases.

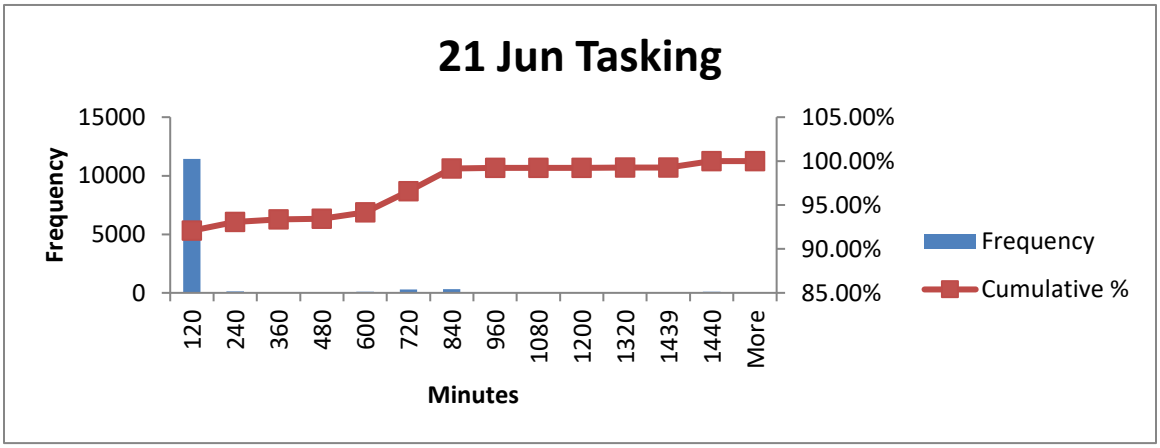

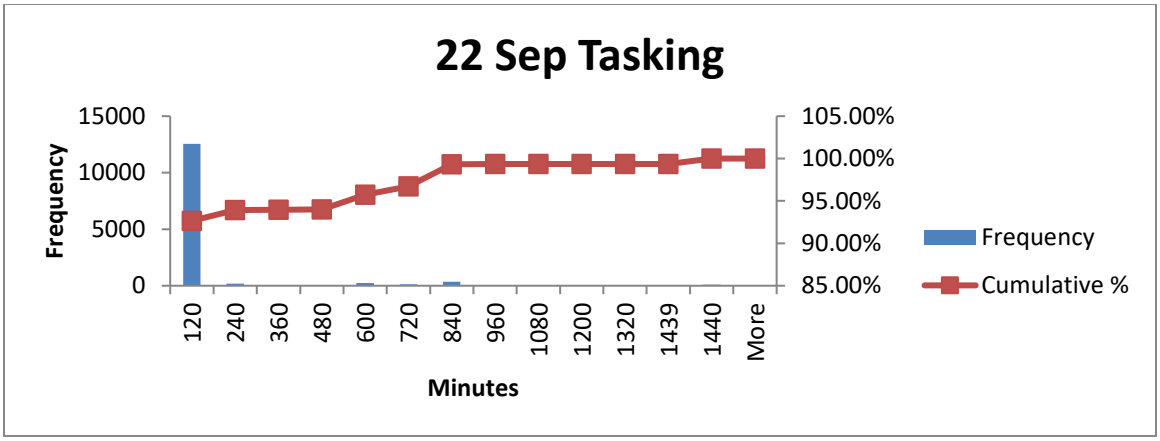

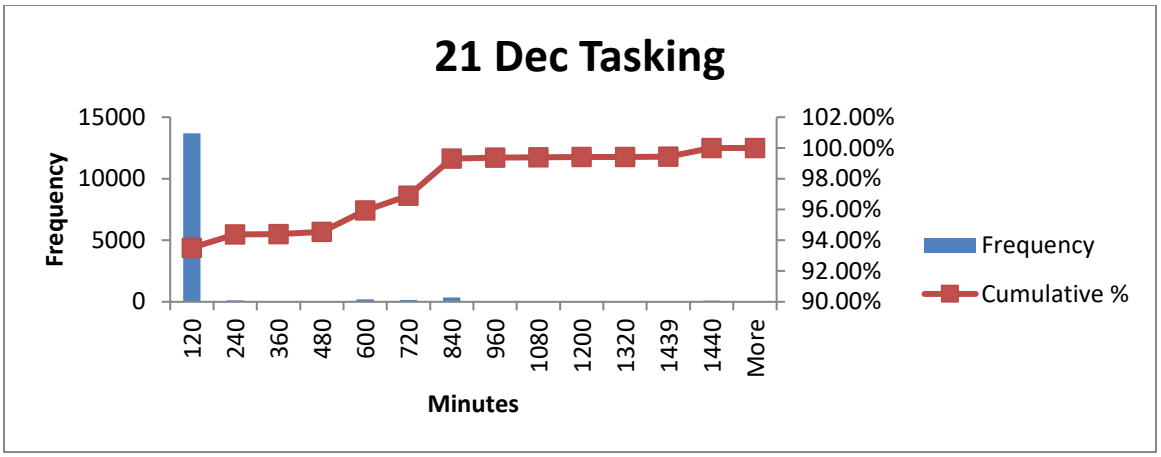
21 Dec Tasking
Frequency
15000
10000
5000
0
102.00%
100.00%
98.00%
96.00%
94.00%
92.00%
90.00%
120
240
360
480
600
720
840
960
1080
1200
1320
1439
1440
More
Minutes
Frequency
Cumulative %

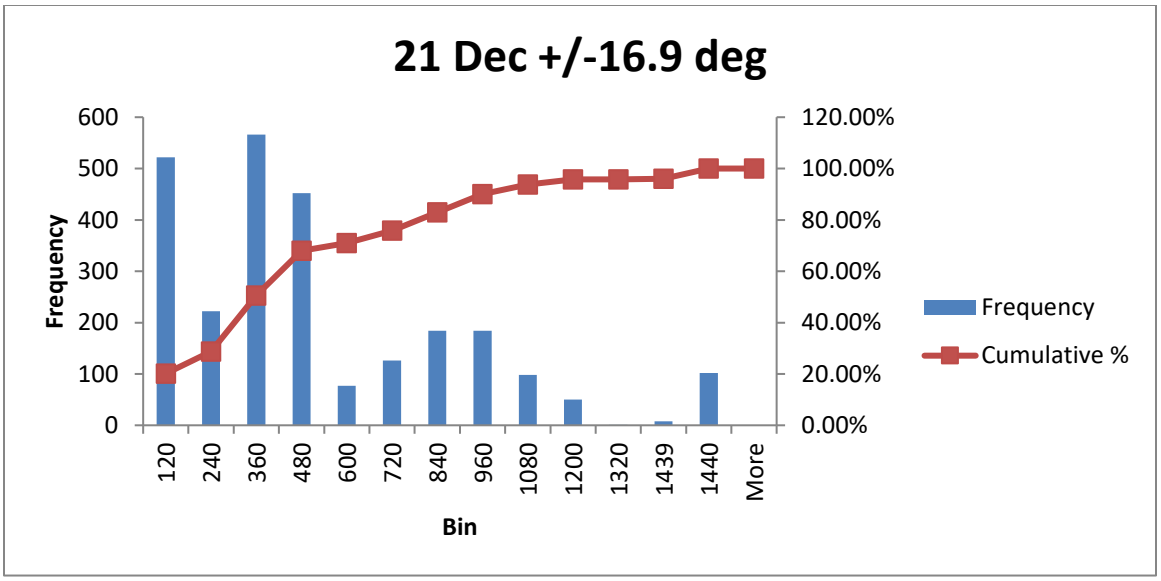
21 Dec +/-16.9 deg
Frequency
600
500
400
300
200
100
0
120.00%
100.00%
80.00%
60.00%
40.00%
20.00%
0.00%
120
240
360
480
600
720
840
960
1080
1200
1320
1439
1440
More
Bin
Frequency
Cumulative %

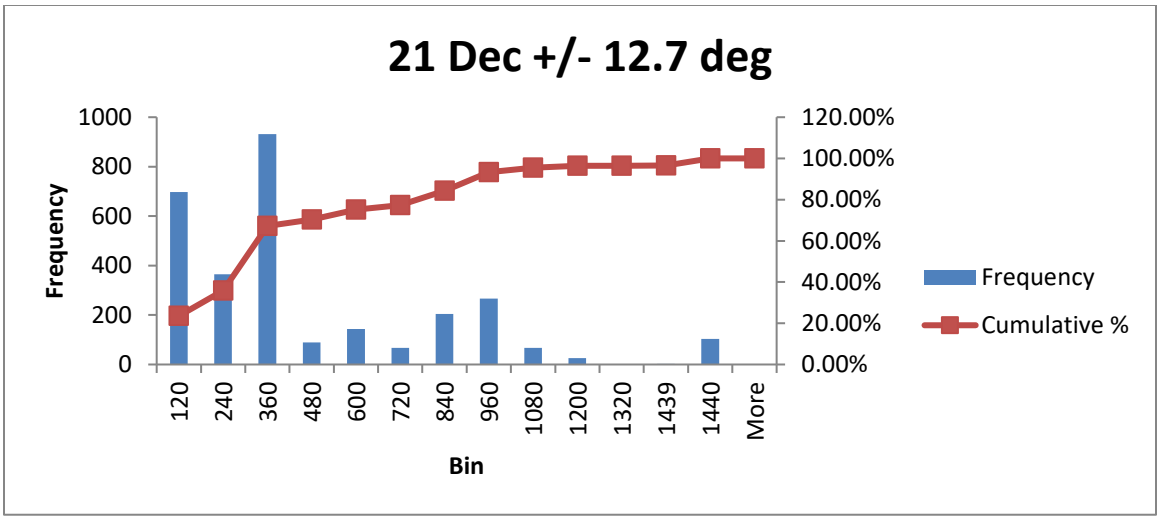
21 Dec +/- 12.7 deg
Frequency
1000
800
600
400
200
0
120.00%
100.00%
80.00%
60.00%
40.00%
20.00%
0.00%
120
240
360
480
600
720
840
960
1080
1200
1320
1439
1440
More
Bin
Frequency
Cumulative %

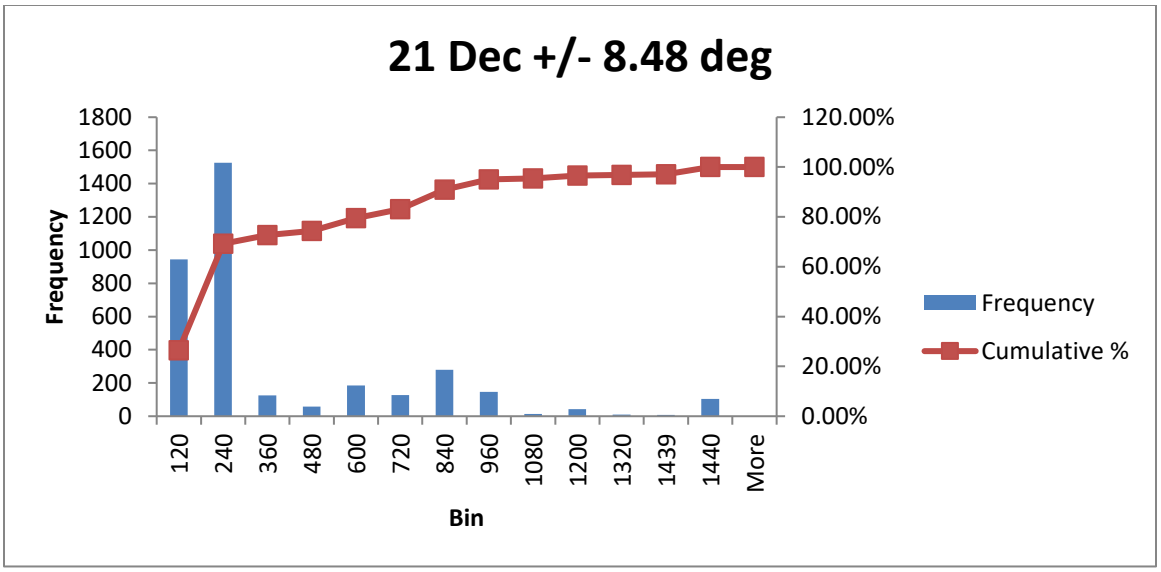
21 Dec +/- 8.48 deg
Frequency
1800
1600
1400
1200
1000
800
600
400
200
0
120.00%
100.00%
80.00%
60.00%
40.00%
20.00%
0.00%
120
240
360
480
600
720
840
960
1080
1200
1320
1439
1440
More
Bin
Frequency
Cumulative %

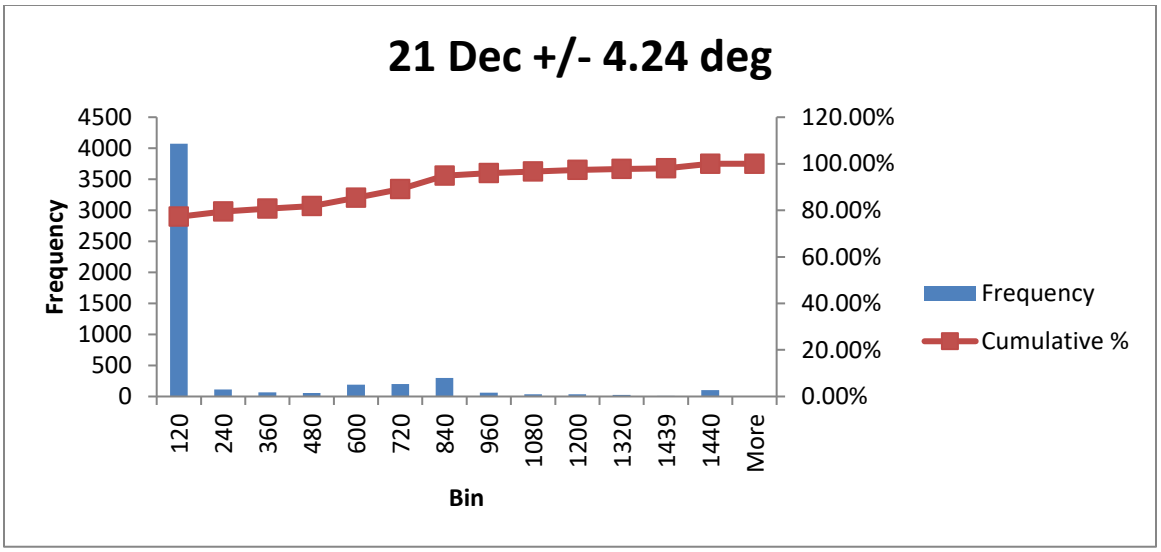
21 Dec +/- 4.24 deg
Frequency
4500
4000
3500
3000
2500
2000
1500
1000
500
0
120.00%
100.00%
80.00%
60.00%
40.00%
20.00%
0.00%
120
240
360
480
600
720
840
960
1080
1200
1320
1439
1440
More
Bin
Frequency
Cumulative %

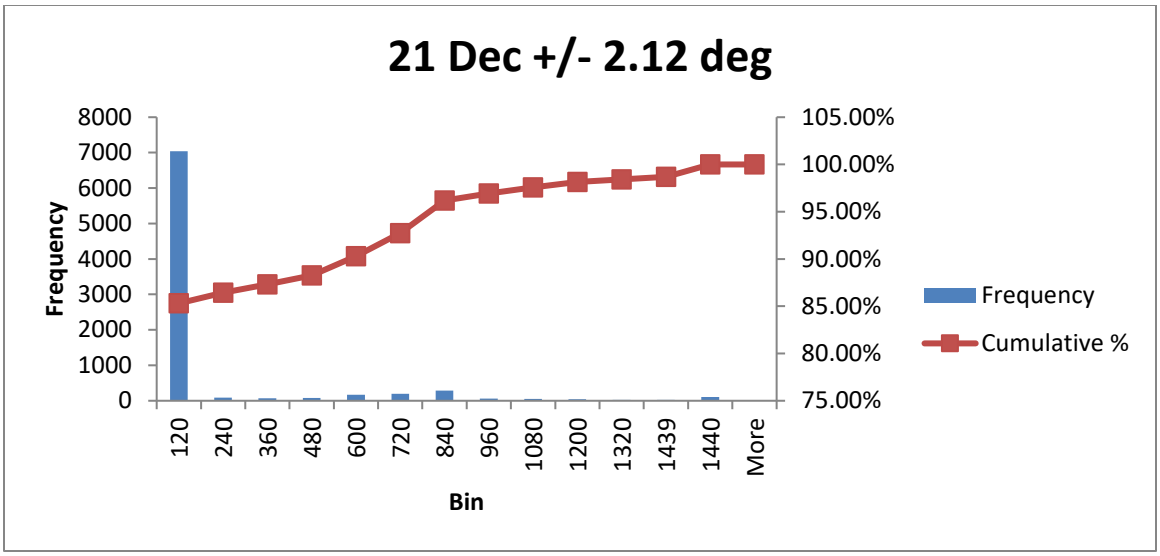
21 Dec +/- 2.12 deg
Frequency
8000
7000
6000
5000
4000
3000
2000
1000
0
105.00%
100.00%
95.00%
90.00%
85.00%
80.00%
75.00%
120
240
360
480
600
720
840
960
1080
1200
1320
1439
1440
More
Bin
Frequency
Cumulative %

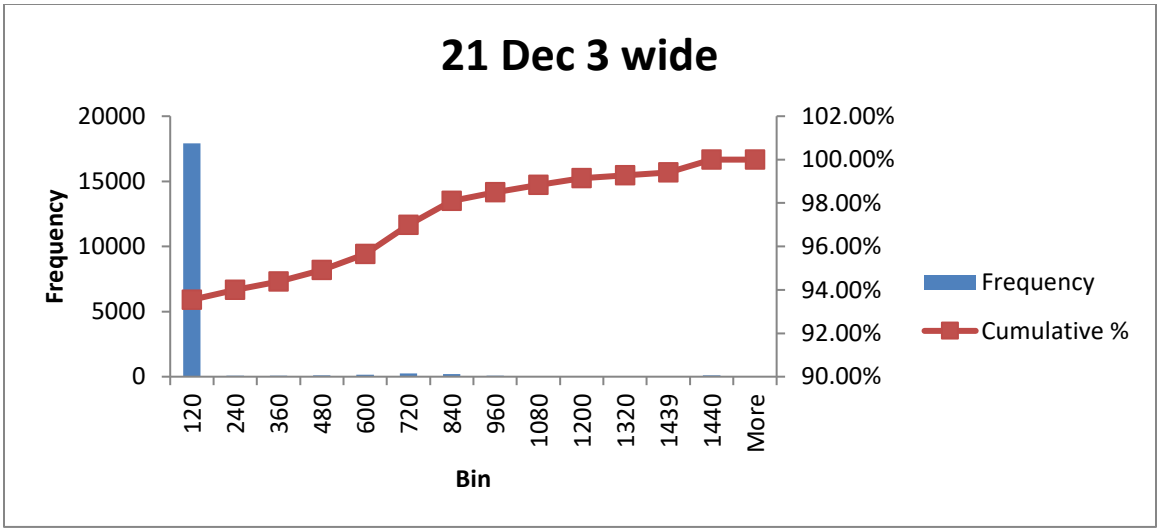
21 Dec 3 wide
Frequency
20000
15000
10000
5000
0
102.00%
100.00%
98.00%
96.00%
94.00%
92.00%
90.00%
120
240
360
480
600
720
840
960
1080
1200
1320
1439
1440
More
Bin
Frequency
Cumulative %

Appendix D

This graph shows the atmospheric transmission vs. elevation angles at Diego Garcia. Atmospheric transmission is factored into the calculation of minimum detectable size. Each observation is taken at a certain elevation which correlates to a transmission factor which is then factored into the visual magnitude calculation.

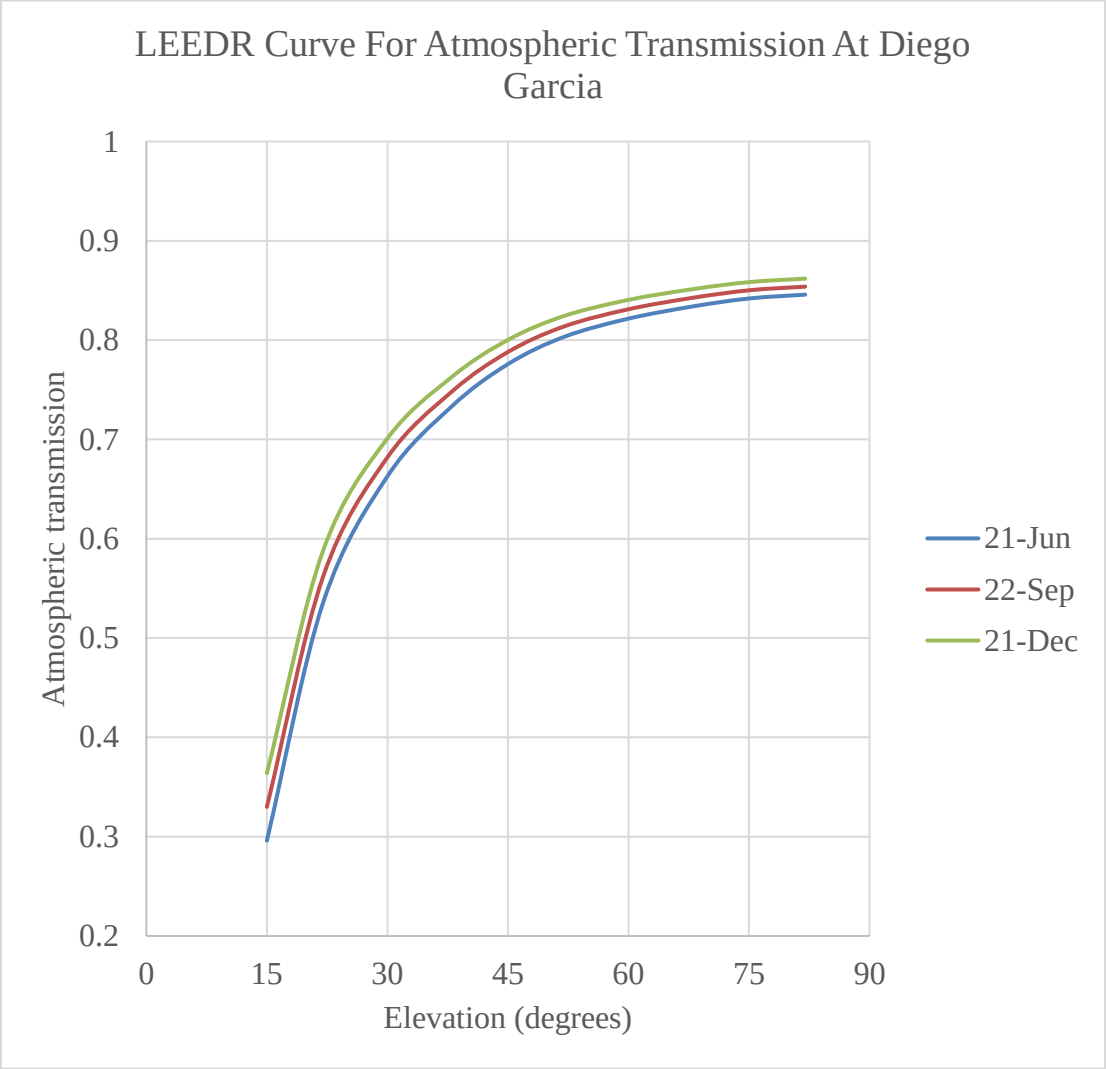

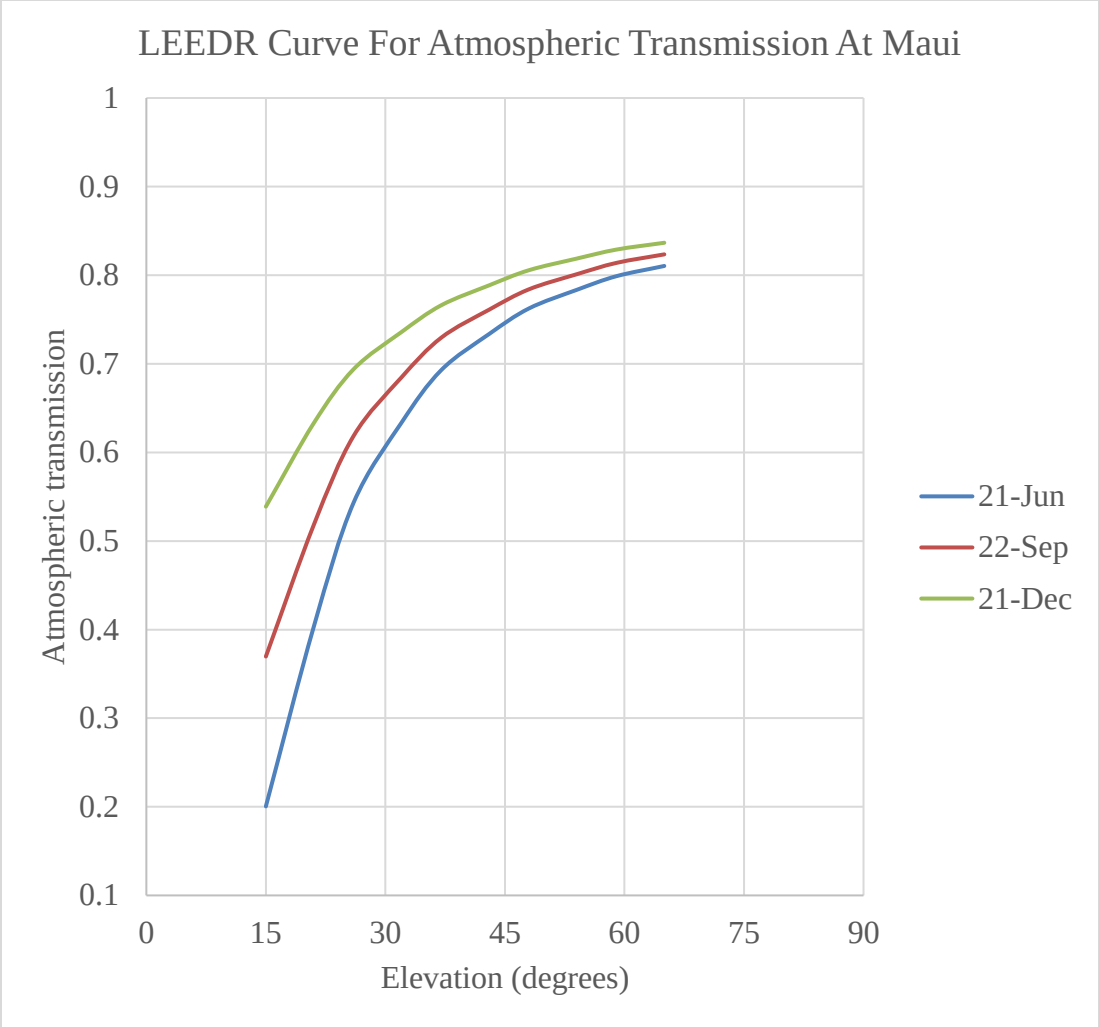
LEEDR Curve For Atmospheric Transmission At Maui
Atmospheric transmission
1
0.9
0.8
0.7
0.6
0.5
0.4
0.3
0.2
0.1
0
15
30
45
60
75
90
Elevation (degrees)
21-Jun
22-Sep
21-Dec

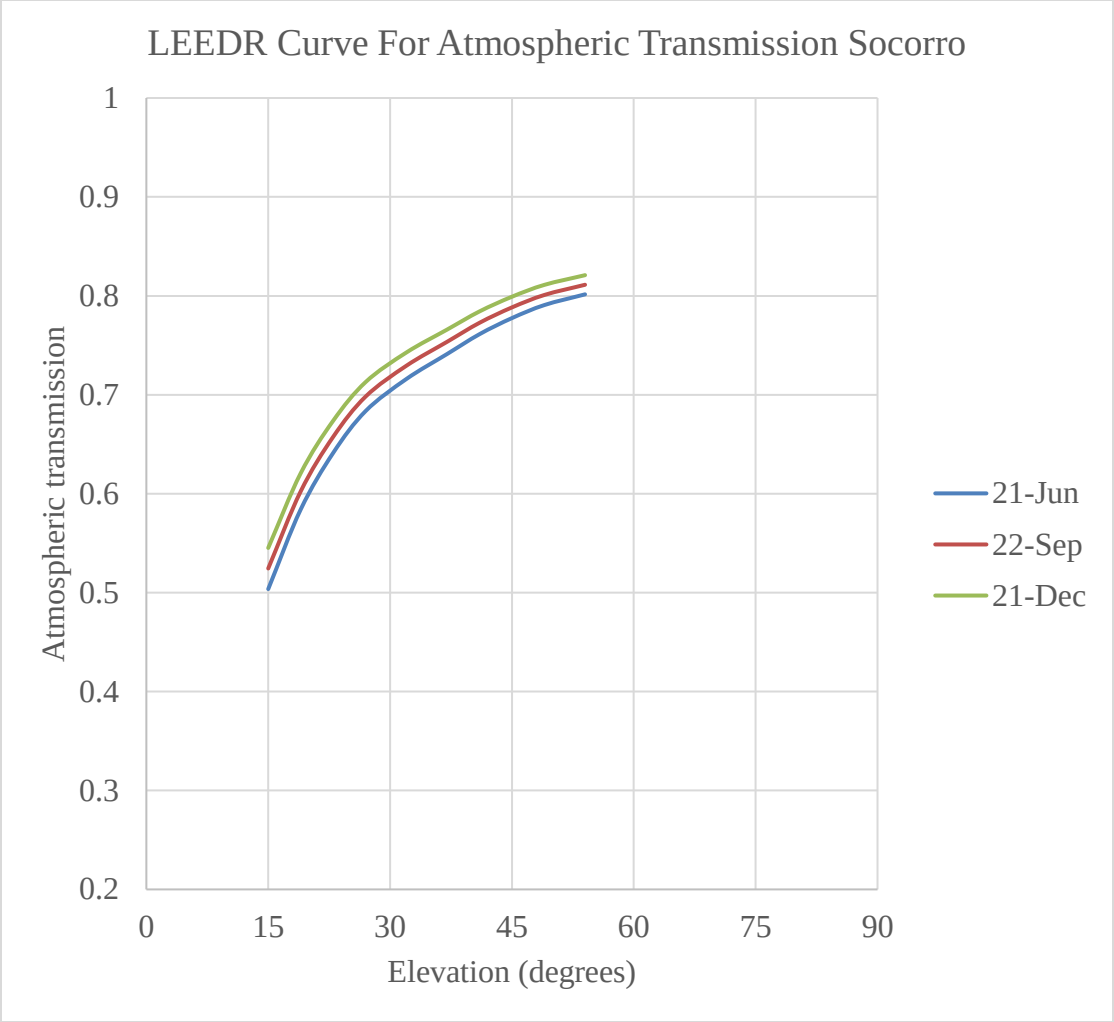
LEEDR Curve For Atmospheric Transmission Socorro
Atmospheric transmission
1
0.9
0.8
0.7
0.6
0.5
0.4
0.3
0.2
0
15
30
45
60
75
90
Elevation (degrees)
21-Jun
22-Sep
21-Dec

Appendix E

The graphs and linear equations below depict how the values were assigned based on performance for the weighted decision matrix.

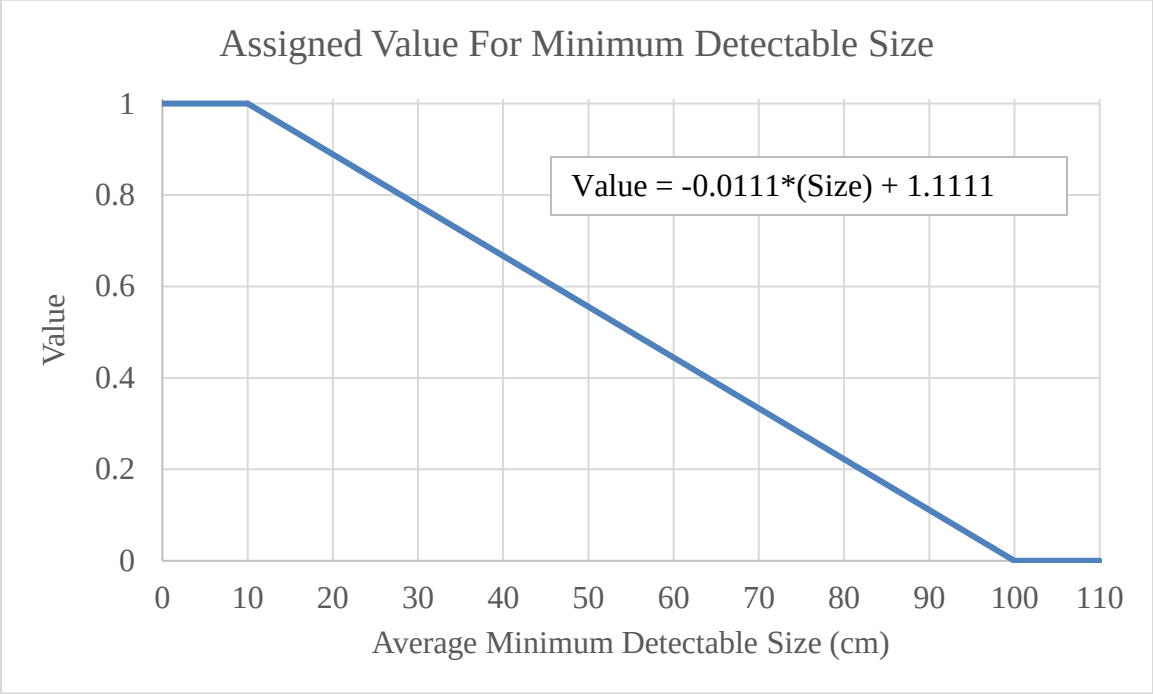

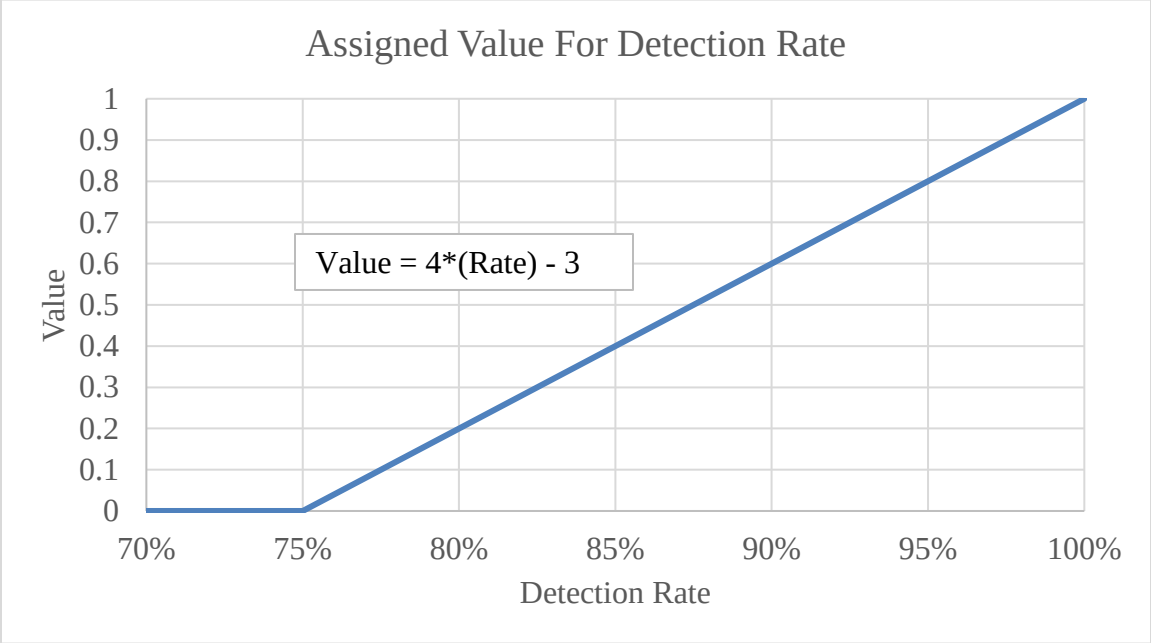

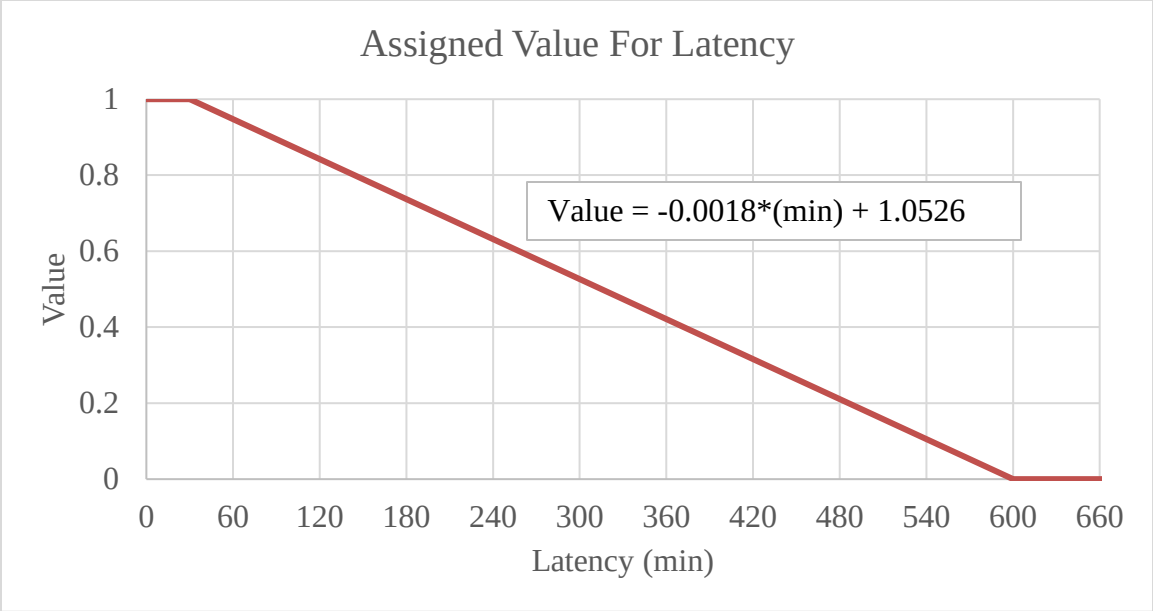
Assigned Value For Latency
Value = -0.0018*(min) + 1.0526
Value
1
0.8
0.6
0.4
0.2
0
0
60
120
180
240
300
360
420
480
540
600
660
Latency (min)

Bibliography

Abercrombly, K. J., Seitzer, P., Barker, E. S., Cowardin, H. M., & Matney, M. J. (2010). Michigan Orbital DEbris Survey Telescope Observations of the Geosynchronous Orbital Debris Environment. *NASA Space Debris Quarterly*, (September), 2007–2009. Retrieved from https://ntrs.nasa.gov/search.jsp?R=20110022976

Ackermann, M. R., Kiziah, R. R., Zimmer, P. C., McGraw, J. T., & Cox, D. D. (2015). A Systematic Examination of Ground-Based and Space-Based Approaches to Optical Detection. In *31st Space Symposium* (pp. 1–46).

AFSPC. (2017a). Geosynchronous Space Situational Awareness Program. *Air Force Space Command*. Retrieved from https://www.afspc.af.mil/About-Us/Fact-Sheets/Display/Article/730802/geosynchronous-space-situational-awareness-program/

AFSPC. (2017b). Ground-Based Electro-Optical Deep Space Surveillance. USAF. Retrieved from https://www.afspc.af.mil/About-Us/Fact-Sheets/Display/Article/249016/ground-based-electro-optical-deep-space-surveillance/

Agapov, V., Molotov, I., & Khutorovsky, Z. (2009). *Analysis of Situation in GEO Protected Region*. *AMOSTECH*. Retrieved from http://www.amostech.com/TechnicalPapers/2009/Orbital_Debris/Agapov.pdf

Alba, O., Payne, D. M., Levan, P. D., Luu, K. K., Spillar, E., Freiwald, W., … Houchard, J. (2017). WENESSA , Wide Eye-Narrow Eye Space Simulation for Situational Awareness. In *Advanced Maui Optical and Space Surveillance Technologies Conference (AMOS)* (p. 9). Retrieved from www.amostech.com

Bates, M. M. S. (n.d.). Capturing Space. USAF. Retrieved from http://airman.dodlive.mil/2016/11/12/capturing-space/

Bernstein, P. (2013). *Background Paper on Space Surveillance Network (SSN) Tasking*.

Beyer, B., & Nelson, N. (2018, June). Space Congestion Threatens to 'Darken Skies.' *National Defense*. Retrieved from http://www.nationaldefensemagazine.org/articles/2018/6/28/viewpoint-space-congestion-threatens-to-darken-skies

Bolden, M., Sydney, P., & Kervin, P. (2011). Pan-STARRRS status and Geo Observations Results. Air Force Research Lab. Retrieved from http://www.dtic.mil/docs/citations/ADA550685

Bruck, R. F., & Copley, R. H. (2014). GEODSS present configuration and potential. *Advanced Maui Optical and Space Surveillance Technologies Conference*.

Choi, J., Jo, J. H., Yim, H., Choi, Y., Son, J., Park, S., … Cho, S. (2015). Analysis of a Simulated Optical GSO Survey Observation for the Effective Maintenance of the Catalogued Satellites and the Orbit Determination Strategy. *Journal of Astronomy and Space Sciences*, *32*(3), 237–245.

Coats, D. R. (2018). *WORLDWIDE THREAT ASSESSMENT of the US INTELLIGENCE COMMUNITY*. Office of Director of National Intelligence. Retrieved from https://www.dni.gov/files/documents/Newsroom/Testimonies/2018-ATA---Unclassified-SSCI.pdf

Cognion, R. L. (2013). Observations and Modeling of GEO Satellites at Large Phase Angles. In *Proceedings from Advanced Maui Optical and Space Surveillance Technologies Conference*. AFSPC SMC. Retrieved from

http://amostech.com/TechnicalPapers/2013/POSTER/COGNION.pdf

Colarco, R. F. (n.d.). Space Surveillance Network Sensor Development, Modification, and Sustainment Programs. In *AMOSTECH*. Retrieved from https://amostech.com/TechnicalPapers/2009/Space_Situational_Awareness/Colarco.pdf

Delligatti, L. (2014). *Sys ML Distilled, A brief guide to the Systems Modeling Language*. Pearson Education, Inc.

Felten, M. (2018). *OPTIMIZATION OF GEOSYNCHRONOUS SPACE SITUATIONAL AWARENESS ARCHITECTURES USING PARALLEL COMPUTATION*. *Air Force Institute of Technology*. M.S Thesis. AFIT-ENV-MS-18-M-202 https://apps.dtic.mil/dtic/tr/fulltext/u2/1056485.pdf

Flohrer, T., Schildknecht, T., & Musci, R. (2008). Proposed strategies for optical observations in a future European Space Surveillance network. *Advances in Space Research*, *41*(7), 1010–1021. https://doi.org/10.1016/j.asr.2007.02.018

Flohrer, T., Schildknecht, T., Musci, R., & Stöveken, E. (2005). Performance estimation for GEO space surveillance. *Advances in Space Research*, *35*(7), 1226–1235. https://doi.org/10.1016/j.asr.2005.03.101

Friedenthal, S., Griego, R., & Sampson, M. (2007). INCOSE model based systems engineering (MBSE) initiative. In *INCOSE 2007 Symposium*. Retrieved from http://www.incose.org/enchantment/docs/07docs/07jul_4mbseroadmap.pdf

Gruss, M. (n.d.). Russian Luch Satellite Relocates — Next to Another Intelsat Craft. Retrieved from https://spacenews.com/russian-luch-satellite-relocates-next-to-another-intelsat-craft/

Johnson, N. L. (2010). Orbital debris: The growing threat to space operations. *NASA Space Debris Quarterly*. Retrieved from https://ntrs.nasa.gov/search.jsp?R=20100004498

JP 3-14, J. P. 3-14 S. (2018). Joint Publication 3-14 Space Operations, (April).

Krag, H., Beltrami-Karlezi, P., Bendisch, J., Klinkrad, H., Rex, D., Rosebrock, J., & Schildknecht, T. (2000). Proof - The extension of ESA's master model to predict debris detections. *Acta Astronautica*, *47*(Nos. 2-9), 687–697. https://doi.org/10.1016/S0094-5765(00)00106-5

Molotov, I., Agapov, V., Kouprianov, V., Titenko, V., Rumyantsev, V., Biryukov, V., … Siniakov, E. (2009). ISON worldwide scientific optical network. In *European Space Agency, (Special Publication) ESA SP* (Vol. 672 SP).

Pomerleau, M. (n.d.). DoD needs to know what's happening in space, general says. Retrieved from https://www.defensenews.com/c2-comms/satellites/2018/06/22/dod-needs-to-know-whats-happening-in-space-general-says/

SAFe Scaled Agile. (2017). Retrieved from https://www.scaledagileframework.com/Model-Based-Systems-Engineering/

Schaefer, B. (1986). Atmospheric Extinction Effects on Stellar Alignmnets. *Archaeoastronomy*, *10*(xvii), S32–S42. Retrieved from https://journals.sagepub.com/doi/pdf/10.1177/002182868601701003

Stern, J., & Wachtel, S. (2017). *GENETIC ALGORITHM OPTIMIZATION OF GEOSYNCHRONOUS EARTH ORBIT SPACE SITUATIONAL AWARENESS SYSTEMS VIA PARALLEL EVALUATION OF EXECUTABLE ARCHITECTURES*. *Air Force Institute of Technology*. M.S. Thesis. AFIT-ENV-MS-17-M-277

Stuckey, L. 2nd L. (USAF). (2011). 20th Space Control Squadron: AFSPC's premier space surveillance squadron. Retrieved from https://www.afspc.af.mil/News/Article-Display/Article/249567/20th-space-control-squadron-afspcs-premier-space-surveillance-squadron/

Thompson, R. E., Colombi, J. M., Black, J., & Ayres, B. J. (2015). Model-Based Conceptual Design Optimization Methods: Disaggregated Weather System Follow-On. *Journal of Spacecraft and Rockets*, *52*(4), 1021–1037. https://doi.org/10.2514/1.A33135

USSTRATCOM. (2010). USSTRATCOM Space Control and Space Surveillance. Retrieved from https://web.archive.org/web/20110817141444/http://www.stratcom.mil/factsheets/USSTRATCOM_Space_Control_and_Space_Surveillance/

REPORT DOCUMENTATION PAGE

Form Approved
OMB No. 074-0188

1. REPORT DATE *(DD-MM-YYYY)*	**2. REPORT TYPE**	**3. DATES COVERED** *(From – To)*
21-03-2019	Master's Thesis	August 2017 – March 2019

TITLE AND SUBTITLE

SEARCH-BASED VS. TASK-BASED SPACE SURVEILLANCE FOR GROUND-BASED TELESCOPES

5a. CONTRACT NUMBER

5b. GRANT NUMBER

5c. PROGRAM ELEMENT NUMBER

6. AUTHOR(S)

Hertwig, Fred D., Captain, USAF

5d. PROJECT NUMBER

5e. TASK NUMBER

5f. WORK UNIT NUMBER

7. PERFORMING ORGANIZATION NAMES(S) AND ADDRESS(S)
Air Force Institute of Technology
Graduate School of Engineering and Management (AFIT/ENY)
2950 Hobson Way, Building 640
WPAFB OH 45433-8865

8. PERFORMING ORGANIZATION REPORT NUMBER

AFIT-ENV-MS-19-M-178

9. SPONSORING/MONITORING AGENCY NAME(S) AND ADDRESS(ES)
Intentionally Left Blank

10. SPONSOR/MONITOR'S ACRONYM(S)

ILB

11. SPONSOR/MONITOR'S REPORT NUMBER(S)

12. DISTRIBUTION/AVAILABILITY STATEMENT
DISTRUBTION STATEMENT A. APPROVED FOR PUBLIC RELEASE; DISTRIBUTION UNLIMITED.

13. SUPPLEMENTARY NOTES
This material is declared a work of the U.S. Government and is not subject to copyright protection in the United States.

14. ABSTRACT
The goal of this thesis was to compare the current task-based space surveillance performance to a search-based method of space surveillance in the GEO belt region. The performance of a ground telescope network, similar to an operational network, was modeled and simulated using AGI's Systems Tool Kit (STK) and Python. The model compared the two methods by simulating 813 Resident Space Objects (RSOs) on 21 Jun, 22 Sep, and 21 Dec. Six different search areas with varying starting positions were also used. Performance metrics for comparing the two methods were smallest detectable size, detection rate, coverage area, and latency. Results have shown that the smallest detectable size average for task-based was 47.6 cm in diameter while search-based methods ranged from 38.3 cm-45.4 cm in diameter. Detection rate for task-based was 100% while the search-based ranged from 91.7%-96.8%. Coverage area for task-based was 46% of the GEO belt and the search-based method ranged from 3.5%-84.4%. Average latency for task-based was 78 minutes and search-based methods ranged from 62-469 minutes. It was found that task-based surveillance performed better in current operational conditions. However, if the number of RSOs is increased there will be a point when search method will have better performance.

15. SUBJECT TERMS
Space Situational Awareness, Geostationary, Modeling and Simulation, Ground-Based Telescopes

16. SECURITY CLASSIFICATION OF:Unclassified			**17. LIMITATION OF ABSTRACT**	**18. NUMBER OF PAGES**	**19a. NAME OF RESPONSIBLE PERSON**
a. REPORT	**b. ABSTRACT**	**c. THIS PAGE**			Dr. John Colombi, AFIT/ENV
U	**U**	**U**	**UU**	95	**19b. TELEPHONE NUMBER** *(Include area code)* (937) 255-3636, ext 3347 (john.colombi@afit.edu)

Standard Form 298 (Rev. 8-98)
Prescribed by ANSI Std. Z39-18